SI Appendix, Supplementary Materials and Methods

Reagents

Recombinant human prokineticin-2 (PROK2) (PeproTech, Cranbury, NJ, USA), U73343, cyclosporine A (CsA), ddAd, protein kinase inhibitor (PKI), amodiaquine (AQ), PKRA7, and C-DIM12 (MedChemExpress, Monmouth Junction, NJ, USA) were purchased and used.

Transcription factor (TF) binding motif analysis

To analyze TF binding motifs, a gene set enrichment analysis (GSEA) approach was employed to compare PROKR1-induced upregulated genes (GSE148443)(1) with gene sets obtained from TRANSFAC (focusing on transcription factors and binding sites) (https://www.gsea-msigdb.org/gsea/). The top 20 overlapping TF binding motif gene sets were identified (FDR $q < 0.05$) and subjected to further analysis.

Cell culture

To culture HEK293T cells (ATCC, Manassas, VA, USA), DMEM medium supplemented with 10% (v/v) FBS and 1% (v/v) antibiotic-antimycotic solution (Gibco, Grand Island, NY, USA) was used and cells were incubated at 37°C with 5% CO_2. C2C12 cells (ATCC) were maintained in DMEM medium with 20% (v/v) FBS and 1% (v/v) antibiotic-antimycotic solution, and differentiated in DMEM medium with 2% (v/v) horse serum (Gibco) and 1% (v/v) antibiotic-antimycotic solution once they reached 80% confluence. Primary human skeletal muscle myoblasts (HSKMC), isolated from Trapezius of a 68-year-old Caucasian male donor, was purchased from PromoCell (Heidelberg, Germany) and differentiated into multinuclear myotubes according to the manufacturer's protocol.

Chromatin immunoprecipitation (ChIP)

HEK293T cells were cross-linked by incubating cells in 1% (w/v) formaldehyde (Sigma-Aldrich, St. Louis, MO, USA) for 15 min at room temperature. Cross-linking was arrested by 5 min of incubation with 125 mM glycine (Sigma-Aldrich). ChIP assay was performed using Magna ChIP™ A/G Chromatin Immunoprecipitation Kit (Sigma-Aldrich). Chromatins were immunoprecipitated overnight at 4°C with antibodies to pCREB (1:50, Cell Signaling Technology, Beverly, MA, USA), nonspecific IgG (Thermo Fisher Scientific, Waltham, MA, USA, 1:250). PCR-based quantification of the precipitated DNA was performed to determine

an association between pCREB and NR4A2 promoter. Data were normalized to input control. All primer sequences are listed in SI Appendix, Dataset S4.

Quantitative real time-PCR (qRT-PCR)

For RNA analysis, we initiated the process by extracting total RNA using the RNeasy mini kit sourced (Qiagen, Hilden, Germany). Subsequently, the obtained RNA underwent reverse transcription, a crucial step carried out with SuperScript III reverse transcriptase (Invitrogen, Waltham, MA, USA). Following this, the resulting cDNA was utilized for quantitative real-time PCR (qRT-PCR), employing specific primers designed for the gene of interest. The quantification of mRNA expression levels was accomplished using the $_{\Delta\Delta}$CT method, with Gapdh mRNA employed as the internal control. For DNA analysis, total DNA was isolated using the DNeasy mini kit (Qiagen). Mitochondrial DNA (mtDNA) levels were assessed using the Mtco2 gene in mice and the MT-TL1 gene in humans, which were then adjusted for normalization against B2m and HBB-B1 genes, respectively. The PCR process involved 40 cycles of denaturation at 95°C for 15 seconds, followed by annealing and extension at 60°C for 1 min, and SYBR green was used as the detection method in real-time PCR systems (Applied Biosystems, Foster City, CA, USA). Additional details about the primers can be found in SI Appendix, Dataset S4.

Luciferase reporter assays

To assess the impact of PROKR1 overexpression or deletion on NR4A2 promoter activity, HEK293T cells were transfected with either a NR4A2 Promoter-Luciferase Reporter construct containing the cAMP-response element (CRE, TGACGTCA) or a NR4A2 Promoter-Luciferase Reporter construct lacking the CRE. The cells were then incubated for 24 hrs, and culture media were collected for luminance measurement. Transcriptional response activity values were expressed as luminance fold changes, and Creb1 promoter activity was measured using the IVISbrite™ D-Luciferin assay kit (PerkinElmer, Waltham, MA, USA).

Western blotting

Cells and tissue were lysed in RIPA buffer (Thermo Fisher Scientific) containing protease inhibitor and phosphatase inhibitor (GenDEPOT, Katy, TX, USA) cocktail. Protein concentrations were determined using the BCA assay kit (Thermo Fisher Scientific). Thirty μg of protein was resolved on 9% (v/v) SDS-PAGE gels and transferred onto PVDF membranes

(0.45 μm, Thermo Fisher Scientific) using a wet transfer apparatus. Membranes were blocked in 5% BSA (Sigma-Aldrich) for 1 hr at room temperature and then probed with primary antibodies against NR4A1 (Santa Cruz, 1:1000), NR4A2 (Santa Cruz, 1:1000), NR4A3 (Santa Cruz, 1:1000), pCREB (Cell Signaling Technology, Beverly, MA, USA, 1:1000), CREB (Cell Signaling Technology, 1:1000), MYH7 (Sigma-Aldrich, 1:1000), MYH4 (Thermo Fisher Scientific, 1:1000), MYH2 (Sigma-Aldrich, 1:1000), PGC1a (Santa Cruz, 1:1000), TFAM (Santa Cruz, 1:1000), and Total OXPHOS WB Antibody Cocktail (Abcam, Cambridge, UK, 1:250) overnight at 4°C. The membranes were washed and incubated with the HRP-goat anti-rabbit and mouse IgG antibody (Thermo Fisher Scientific, 1:5000) for 1 hr at room temperature. Protein bands were detected using an ECL substrate (BioRad, Berkeley, CA, USA) and imaged using an Image J (NIH, USA) software. ACTB (Santa Cruz) was used as a loading control for normalization of protein loading.

Enzyme-linked immunosorbent assay (ELISA)

Quantification of phosphorylated CREB to total CREB ratios using the pCREB/CREB ELISA kit (R&D Systems, Minneapolis, MN, USA) and Insulin ELISA kit (Crystal Chem, Downers Grove, IL, USA) according to the manufacturer's instructions and signals were obtained with Cytation 5 (Agilent Technologies, Santa Clara, CA, USA).

Immunocytochemistry

C2C12 and HSKMC-derived myotubes were fixed in 4% (w/v) paraformaldehyde (Biosesang, Seoul, Korea) and permeabilized with TRIS-buffered saline containing 0.1% (v/v) Tween 20 (Sigma-Aldrich). Primary antibodies, including anti-MYH7 (Sigma-Aldrich, 1:1000), anti-MYH4 (Thermo Fisher Scientific, 1:100), and anti-MYH2 (Sigma-Aldrich, 1:100), were used to target specific muscle fibers. After primary antibody incubation, cells were incubated with a goat anti-mouse Alexa-488 secondary antibody (Thermo Fisher Scientific, 1:1000). The nuclei were counterstained using DAPI (Sigma-Aldrich). The fluorescence images were captured using Cytation 5 (Agilent Technologies) and the fluorescence intensity of the immuno-labeled cells was normalized to nuclei.

siRNA transfection and AAV transduction

C2C12 cells were cultured in 24-well plates at a density of 10^4 cells per well. After 24 hrs, the cells were treated with either AAV6-PROKR1 or AAV6-NR4A2 (VectorBuilder, Chicago, IL,

USA) at a multiplicity of infection (MOI) of 1×10^4 viral genomes per cell. To knock-down Prokr1 or Nr4a2, C2C12 cells were transfected with 50 μM of siRNAs targeting either Prokr1 or Nr4a2 (Bioneer, Daejeon, Korea) using Lipofectamine RNAiMAX Reagent (Thermo Fisher Scientific). The cells were then maintained for five days in a differentiation medium containing 2% (v/v) horse serum. AAV6-mock or siRNA-Scramble (Bioneer) was used as controls.

Mitochondria quantification

Cell and muscle tissues were subjected to staining procedures for visualization with MitoTracker Red for mitochondria, Phalloidin-488 for actin filaments (Cell Signaling Technology), and DAPI for nuclei (Vector Laboratories, Inc.). The fluorescence intensity was measured using the Cytation 5 (Agilent Technologies). Image J software was applied to quantify the number of mitochondria, normalized by the fluorescence intensity of the nuclear stain.

Fatty acid oxidation (FAO)

FAO activity was assessed using the Fatty Acid Oxidation Assay kit (AssayGenie, Dublin, Ireland) as per the manufacturer's instructions. C2C12 and HSKMC cell lysates were centrifuged at maximum speed for 5 min, and the resulting supernatant was collected and transferred to a 96-well plate (Corning). To each well, 50 μL of reaction solution was added, and the mixture was then incubated at 37°C for 2 hrs. The measurement of the redox product, iodonitrotetrazolium-formazan, was carried out at 492 nm to determine the level of FAO activity.

Lactate measurement

The L-lactate levels in the media of C2C12 and HSKMC cells were measured after 24 hrs using Lactate assay kit (Cayman Chemicals, Ann Arbor, MI, USA). The cells were seeded at a density of 10^4 cells/well in a 96-well plate with 100 μL of media. The collected samples were analyzed using the kit's instructions, and the readings were recorded and calculated.

Animals

C57BL6/N mice were bred and maintained in a specific pathogen-free (SPF) facility with a 12-hr light/dark cycle and controlled temperature and humidity. The mice were fed either a normal chow diet (N) or a high-fat diet (H) with 60% of calories derived from fat (Research Diets,

New Brunswick, NJ, USA). Mice were housed in cages with five animals each and their body weight and food intake for each mouse (g/day/head) were measured weekly from 6 to 21 weeks of age. The mice were weighed at the same time of day to minimize variability. The research involving animals was conducted at Seoul National University and received ethical approval from the Institutional Animal Care and Use Committees (IACUC) under the reference number SNU-220504-2-1. All procedures were performed in compliance with the approved guidelines.

Generation of Prokr1 knock-out mouse

Fertilized one-cell embryos were collected from C57BL6/N mice (Koatech, Pyeongtaek, Korea). SpCas9 protein at 200 ng/μL (Toolgen Inc. in Seoul, Korea) and 50 ng/μL of sgRNA were introduced into the embryos using Neon Electroporator (Thermo Fisher Scientific). The embryos were then transferred into the oviducts of surrogate ICR female mice (Koatech), and the founder mice were verified through PCR genotyping and Sanger sequencing. Prokr1 heterozygous male and female mice were bred and litters of wild-type, heterozygous, and homozygous knock-out mice were used for the study. Additional details about the primers or sgRNA can be found in SI Appendix, Dataset S4.

Dual energy X-ray absorptiometry (DEXA)

Body composition was assessed using the InAlyzer DEXA system (Medikors, Seongnam, Korea). For this evaluation, 25 weeks of age mice were anesthetized with a 300 mg/kg intraperitoneal injection of avertin (Sigma-Aldrich). The InAlyzer system utilizes radiation absorption measurements to precisely determine material density by emitting both low and high-energy X-ray beams. These X-rays are then detected and analyzed by the InAlyzer software, which computes essential body composition parameters such as fat mass, lean mass, and body fat percentage.

Glucose tolerance and insulin tolerance tests (GTT and ITT)

GTT and ITT tests were performed on 6 hr-fasted mice 18 or 19 weeks of age. During the GTT, mice were orally administered 1.5 g/kg of glucose (Sigma-Aldrich), and their blood glucose levels were monitored for 120 min using a glucometer (Roche, Basel, Switzerland). In the ITT, 30 min after the oral glucose administration, mice were intraperitoneally injected with 1.0 U/kg of insulin (Sigma-Aldrich), and blood glucose levels were measured. The area under the curve

(AUC) for glucose levels during both the GTT and ITT was calculated using Prism software (GraphPad, San Diego, CA, USA).

Non-esterified fatty acid (NEFA) measurement

Blood samples were collected from 6 hr-fasted mice using EDTA-coated tubes and promptly placed on ice to maintain their integrity. Subsequently, the samples were centrifuged at 4,000 rpm for a duration of 10 min. To determine the levels of serum non-esterified fatty acids (NEFA), a LabAssay NEFA kit (Wako, Osaka, Japan) was employed following the guidelines provided by the manufacturer.

Indirect calorimetry

Mice at 25 weeks of age were individually placed in metabolic cages (TSE Systems, Berlin, Germany). Following a 48-hr acclimatization period, the mice were continuously monitored for 72 hrs with unrestricted access to food. Oxygen consumption (VO_2) and carbon dioxide production (VCO_2) were recorded for each mouse and applied to calculate energy expenditure (EE) using the Weir equation [EE (kcal/day) = (VO_2 × 3.941 + VCO_2 × 1.106) × 1440]. Ambulatory activity was assessed by tallying interruptions detected by a multi-dimensional infrared beam system along both the X and Y axes. For analysis purposes, data from the final 48 hrs of indirect calorimetry and ambulatory activity were utilized.

Grip strength

Mice at 23 weeks of age were evaluated for their grip strength using a digital grip-strength meter (BIOSEB, Vitrolles, France). To perform the test, the mice were placed over the grid with their bodies kept horizontal, ensuring that only their four paws made contact with the grid. The mouse's tail was gently pulled to encourage a strong grip on the top part of the grid while maintaining a horizontal body position. To ensure accuracy, each mouse underwent three trials, and the highest force achieved was then adjusted based on the bodyweight. The investigators conducting the grip strength study were blinded to specific information or variables.

Hematoxylin and eosin (H&E) Staining

Skeletal muscle and white adipose tissues were fixed in 4% neutral buffered formalin (Sigma-Aldrich) for 24 hrs, then dehydrated using ethanol (Sigma-Aldrich), rinsed in xylene (Thermo Fisher Scientific), and embedded in paraffin wax. Tissue slices, 5 μm thick, were created and

placed onto glass slides. These sections underwent H&E staining (Sigma-Aldrich), involving deparaffinization, hematoxylin staining, rinsing, eosin counterstaining, dehydration, washing, and mounting. The stained sections were observed using a Cytation 5 imaging system (Agilent Technologies).

Immunohistochemistry (IHC)

Following necropsy, skeletal muscle tissue was promptly frozen using isopentane (Thermo Fisher Scientific) and cooled with liquid nitrogen. Frozen sections, each 10 μm thick, were then created and placed onto slides. The sections were then incubated overnight with primary antibodies against MyHC1 (DSHB, lowa City, IA, USA, 1:100), MyHC2a (DSHB, 1:100), and MyHC2b (DSHB, 1:50) followed by incubation with secondary antibodies: Alexa Fluor 350-conjugated goat anti-mouse IgG2b (Thermo Fisher Scientific, 1:100), Alexa Fluor 488-conjugated goat anti-mouse IgG1 (Thermo Fisher Scientific, 1:100), and Alexa Fluor 594-conjugated goat anti-mouse IgM (Thermo Fisher Scientific, 1:100). The muscle sections were mounted and captured using the Cytation 5 imaging system (Agilent Technologies). Muscle fiber type composition count and area were analyzed using Gen 5 software (Agilent Technologies) with automatic recognition based on color.

Prokr1 rescue in mice

AAV6-CMV-PROKR1 at a MOI of 1×10^{10} viral genomes (VectorBuilder) diluted in 50 μL of PBS was injected into the left leg muscles (tibialis anterior, quadriceps, gastrocnemius) of 18 weeks old Prokr1-deficient male mice. AAV-mock was injected into the right leg muscles of the same mice. For comparison, 10 μM of siRNA-Prokr1 (Bioneer) diluted in 50 μL of PBS was injected into the left leg muscles of 8 weeks old Prokr1 wild-type male mice, and siRNA-scramble into the right leg muscles. One week after injection, mice were sacrificed and the leg muscle tissues were collected and subjected to further analyses.

Statistical analysis

All data were analyzed using Prism software (GraphPad Software). The test methods used depending on the homogeneity of variance of the data and the number of groups are described in the figure legends. A p-value of less than 0.05 was considered statistically significant. Unless otherwise noted, values are reported as mean ± standard deviation (SD).

References

1. J. Mok *et al.*, Prokineticin receptor 1 ameliorates insulin resistance in skeletal muscle. *FASEB J* **35**, e21179 (2021).

SI Appendix, Supplementary Figure Legends

SI Appendix, Fig. S1. Relative mRNA levels of *NR4A* family genes

PROKR1-TG is PROKR1 overexpressing HEK293T cells, PROKR1-KO for PROKR1 knock-out cells. PROK2 is PROKR1 natural agonist. Values are mean ± SD (n = 3). ***$p < 0.001$, unpaired two-tailed Student *t*-test.

SI Appendix, Fig. S2. Expressional dynamics between pCREB and NR4A2

Time-course Western blotting and quantification of pCREB and NR4A2 in C2C12 and HSKMC myotubes after PROK2 treatment (0, 5, 10, 20, 40 min, 1, 2, 4, 8, 12 hr). Values are mean ± SD (n = 3). *$p < 0.05$, **$p < 0.01$, ***$p < 0.05$ vs. 0 hr, one-way ANOVA followed by Dunnett's post-hoc analysis.

SI Appendix, Fig. S3. Relative mRNA levels of oxidative muscle fiber marker genes

C2C12 is mouse myocytes, HSKMC for human myocytes. PROK2 is PROKR1 natural agonist. *Myh7, Tnnc1*, and *Tnni1* are used for oxidative muscle fibers, *Myh4, Myh2*, and *Tnni2* for glycolytic muscle fibers. Values are mean ± SD (n = 3). *$p < 0.05$, **$p < 0.01$, ***$p < 0.001$, unpaired two-tailed Student *t*-test.

SI Appendix, Fig. S4. AAV serotype screening in human myotubes

Green fluorescence indicates AAV transduced human myofibers. Values are mean ± SD (n = 5 ~ 6). Scale bar is 200 μm.

SI Appendix, Fig. S5. siRNA screening in mouse myotubes

Different combination of siRNA against *Prokr1* or *Nr4a2* is used. Values are mean ± SD (n = 3). **$p < 0.01$, ***$p < 0.001$ vs Mock control, one-way ANOVA followed by Dunnett's post-hoc analysis.

SI Appendix, Fig. S6. Relative mRNA levels of mitochondrial marker genes

C2C12 is mouse myocytes, HSKMC for human myocytes. PROK2 is PROKR1 natural agonist. Values are mean ± SD (n = 3). *$p < 0.05$, **$p < 0.01$, ***$p < 0.001$, unpaired two-tailed Student *t*-test.

SI Appendix, Fig. S7. **Western blotting of respiratory chain complexes**

Western blotting of respiratory chain complexes. C2C12 is mouse myocytes, HSKMC for human myocytes. PROK2 is PROKR1 natural agonist (n = 3).

SI Appendix, Fig. S8. Prokr1 knock-out mouse generation

A. Schematic diagram of Prokr1 deletion using CRISPR/Cas9. Eight bases in exon 2 of the 12.15 kb mouse Prokr1 gene are deleted by CRISPR/Cas9. In the DNA sequences presented, *italicized characters* denote the target sequence of the sgRNA, <u>underlined</u> denotes the PAM sequence, and **bold** denotes the deleted sequence. The red arrow at the top of exon 2 indicates the binding site of the sequencing primer, and the blue arrow at the bottom indicates the binding site of the PCR primer for validating the homozygous KO. The amino acid sequences of the wild-type and frameshifted Prokr1 proteins are presented below. **B**. T7E1 assay. M: DNA size marker, WT: Prokr1 wild-type mouse, Het: Prokr1 heterozygous knock-out mouse, Hom: Prokr1 homozygous knock-out mouse. **C**. Deletion-specific PCR. An amplicon of 112 bp is not observed in a Prokr1 homozygouse knock-out mouse sample by primers designed to recognize the deleted bases. **D**. Prokr1 protein expression. Western blotting shows Prokr1 protein expression in gastrocnemius muscle (Gastroc), soleus muscle, brain, inguinal fat, epididymal fat, and liver.

SI Appendix, Fig. S9. **Body weight changes**

Prokr1 genotype effect on body weight changes in mice. Values are mean ± SD (male, n = 6 ~ 7, female, n = 4 ~ 7). N means normal chow, H for high fat diet, $^{+/+}$ for *Prokr1* wild-type mice, $^{+/-}$ *Prokr1* heterozygous knock-out mice, $^{-/-}$ for *Prokr1* homozygous knock-out mice. ***$p <$ 0.001 vs $H^{+/+}$, one-way ANOVA followed by Dunnett's post-hoc analysis.

SI Appendix, Fig. S10. Food consumption

Prokr1 genotype effect on food consumption in mice. Values are mean ± SD (male, n = 6 ~ 7, female, n = 4 ~ 7). N means normal chow, H for high fat diet, $^{+/+}$ for *Prokr1* wild-type mice, $^{+/-}$ *Prokr1* heterozygous knock-out mice, $^{-/-}$ for *Prokr1* homozygous knock-out mice.

SI Appendix, Fig. S11. Absolute and relative organ weights of male mice

Prokr1 genotype effect on organ weights. N means normal chow, H for high fat diet, $^{+/+}$ for *Prokr1* wild-type mice, $^{+/-}$ *Prokr1* heterozygous knock-out mice, $^{-/-}$ for *Prokr1* homozygous

knock-out mice. Values are mean ± SD (n = 5 ~ 6). *$p < 0.05$, **$p < 0.01$ vs. $N^{+/+}$, $^{\dagger}p < 0.05$, $^{\dagger\dagger}p < 0.01$, $^{\dagger\dagger\dagger}p < 0.001$ vs. $H^{+/+}$, one-way ANOVA followed by Dunnett's post-hoc analysis, $^{\#}p < 0.05$, $^{\#\#}p < 0.01$, $^{\#\#\#}p < 0.001$ vs. $N^{+/+}$, unpaired two-tailed Student *t*-test.

SI Appendix, Fig. S12. Histology of male adipose tissues

Prokr1 genotype effect on adipose tissue histology. N means normal chow, H for high fat diet, $^{+/+}$ for *Prokr1* wild-type mice, $^{+/-}$ *Prokr1* heterozygous knock-out mice, $^{-/-}$ for *Prokr1* homozygous knock-out mice. Scale bar is 200 μm.

SI Appendix, Fig. S13. Histology of male skeletal muscle tissues

Prokr1 genotype effect on muscle tissue histology. N means normal chow, H for high fat diet, $^{+/+}$ for *Prokr1* wild-type mice, $^{+/-}$ *Prokr1* heterozygous knock-out mice, $^{-/-}$ for *Prokr1* homozygous knock-out mice. Scale bar is 200 μm.

SI Appendix, Fig. S14. Capillary distribution in male muscle tissues

Capillaries in unit area (0.48 mm^2) are counted in the gastrocnemius and soleus muscle tissues. N means normal chow, H for high fat diet, $^{+/+}$ for *Prokr1* wild-type mice, $^{+/-}$ for *Prokr1* heterozygous knock-out mice, $^{-/-}$ for *Prokr1* homozygous knock-out mice. Values indicate mean ± SD (n = 3). $^{\dagger\dagger}p < 0.01$, $^{\dagger\dagger\dagger}p < 0.001$ vs. $H^{+/+}$, one-way ANOVA followed by Dunnett's post-hoc analysis, $^{\#}p < 0.05$ vs. $N^{+/+}$, unpaired two-tailed Student *t*-test.

SI Appendix, Fig. S15. Fiber counts in male muscle tissues

Total fiber counts per unit area (0.48 mm^2) in the gastrocnemius and soleus muscle tissue are presented. N means normal chow, H for high fat diet, $^{+/+}$ for *Prokr1* wild-type mice, $^{+/-}$ for *Prokr1* heterozygous knock-out mice, $^{-/-}$ for *Prokr1* homozygous knock-out mice. Values indicate mean ± SD (n = 4~6). $^{\dagger}p < 0.05$, $^{\dagger\dagger}p < 0.01$ vs. $H^{+/+}$, one-way ANOVA followed by Dunnett's post-hoc analysis, $^{\#\#}p < 0.01$ vs. $N^{+/+}$, unpaired two-tailed Student *t*-test.

SI Appendix, Fig. S16. Effect of Prokr1 genotype on respiratory exchange ratio (RER) and energy expenditure (EE) in male mice

RER (VCO_2/VO_2) and EE (kcal/hr/kg) measured by indirect calorimetry during two light (white area) and dark cycles (gray area) of 48 hrs are presented. N means normal chow, H for high fat diet, $^{+/+}$ for *Prokr1* wild-type mice, $^{+/-}$ *Prokr1* heterozygous knock-out mice, $^{-/-}$ for

Prokr1 homozygous knock-out mice. Values indicate mean ± SD (n = 3).

SI Appendix, Fig. S17. Heart analyses of male mice

A. Histological examination of the heart. LV stands for left ventricular wall, IVS for interventricular septum. Scale bar is 5 mm. **B**. Structural analysis of the heart. Relative heart weight (mg/g bw), LV wall width (μm/g bw), and IVS width (μm/g bw) are presented. **C**. Functional analysis of the heart. Systolic and diastolic blood pressure (bp) are presented. WT means *Prokr1* wild-type mice, KO for *Prokr1* knock-out mice. Values indicate mean ± SD (n = 3). $p < 0.05$ vs. WT, two-side Student *t*-test.

SI Appendix, Fig. S18. **Effect of Prokr1 on muscle fiber composition and signaling activity in the soleus muscle of male mice**

A. Western blotting and quantification of muscle fiber markers (n = 3). **B**. Immunofluorescence staining and quantification of MyHC-I (blue), MyHC-IIA (green), and MyHC-IIB/X (red/black) proteins (n = 5). Scale bar is 100 μm. **C**. MitoTracker staining and quantification of mitochondrial mass (n = 5 ~ 7). **D**. Western blotting and quantification of Prokr1 signaling proteins (n = 3). Values are mean ± SD. $^{*}p < 0.05$, $^{**}p < 0.01$, $^{***}p < 0.001$ vs. $N^{+/+}$, $^{\dagger}p < 0.05$, $^{\dagger\dagger}p < 0.01$, $^{\dagger\dagger\dagger}p < 0.001$ vs. $H^{+/+}$, one-way ANOVA followed by Dunnett's post-hoc analysis$^{\#\#}p < 0.01$, $^{\#\#\#}p < 0.001$ vs. $N^{+/+}$, unpaired two-tailed Student *t*-test.

SI Appendix, Fig. S19. Fiber size distribution by fiber type in male muscle tissues

Cross-sectional area of each muscle fiber type in the gastrocnemius (gastroc) and soleus muscle tissues are presented. Scatter plots indicate individual cross-sectional area combined with mean ± SD (n = 13~131). N means normal chow, H for high fat diet, $^{+/+}$ for *Prokr1* wild-type mice, $^{+/-}$ for *Prokr1* heterozygous knock-out mice, $^{-/-}$ for *Prokr1* homozygous knock-out mice. $^{*}p < 0.05$, $^{***}p < 0.001$ vs. $N^{+/+}$, $^{\dagger}p < 0.05$, $^{\dagger\dagger\dagger}p < 0.001$ vs. $H^{+/+}$, one-way ANOVA followed by Dunnett's post-hoc analysis, $^{\#\#}p < 0.01$, $^{\#\#\#}p < 0.001$ vs. $N^{+/+}$, unpaired two-tailed Student *t*-test.

SI Appendix, Fig. S20. Mitochondria mass analysis in male muscles

MitoTracker analysis in the soleus and gastrocnemius muscle tissue. Red indicates mitochondria, blue for nuclei. N means normal chow, H for high fat diet, $^{+/+}$ for *Prokr1* wild-type mice, $^{+/-}$ *Prokr1* heterozygous knock-out mice, $^{-/-}$ for *Prokr1* homozygous knock-out mice.

Scale bar is 100 μm.

SI Appendix, Fig. S21. **Western blotting of respiratory chain complexes in male muscles**
Western blotting of oxidative phosphorylation complexes in the soleus and gastrocnemius muscles (n = 3). N means normal chow, H for high fat diet, $^{+/+}$ for *Prokr1* wild-type mice, $^{+/-}$ *Prokr1* heterozygous knock-out mice, $^{-/-}$ for *Prokr1* homozygous knock-out mice.

SI Appendix, Fig. S22. Quantification of respiratory chain complexes in male muscles
Quantification of oxidative phosphorylation complexes in the soleus and gastrocnemius muscles. N means normal chow, H for high fat diet, $^{+/+}$ for *Prokr1* wild-type mice, $^{+/-}$ for *Prokr1* heterozygous knock-out mice, $^{-/-}$ for *Prokr1* homozygous knock-out mice. Values are mean ± SD (n = 3). *$p < 0.05$, ***$p < 0.001$ vs. $N^{+/+}$, $^{\dagger}p < 0.05$, $^{\dagger\dagger\dagger}p < 0.001$ vs. $H^{+/+}$, one-way ANOVA followed by Dunnett's post-hoc analysis.

SI Appendix, Fig. S23. **Western blotting of Prokr1 signaling pathway in male muscles**
Western blotting of Prokr1 signaling pathway in soleus and gastrocnemius muscle tissues. N means normal chow, H for high fat diet, $^{+/+}$ for *Prokr1* wild-type mice, $^{+/-}$ for *Prokr1* heterozygous knock-out mice, $^{-/-}$ for *Prokr1* homozygous knock-out mice.

SI Appendix, Fig. S24. Effect of Prokr1 on muscle fiber composition and signaling activity in male skeletal muscles
In the quadriceps, tibialis anterior, and soleus muscles after AAV-PROKR1 or siRNA-Prokr1 injection, the expression levels Prokr1 signaling proteins and muscle fiber markers are depicted (n = 3). Immunofluorescence staining and composition of MyHC-I (blue), MyHC-IIA (green), and MyHC-IIB/X (red/black)-positive fibers (n = 4) are followed. Scale bar is 100 μm. Values are mean ± SD. *$p < 0.05$, **$p < 0.01$, ***$p < 0.05$ vs. AAV-mock or siRNA-scramble controls, unpaired two-tailed Student *t*-test.

SI Appendix, Fig. S25. ChIP-PCR analysis of pCreb binding site in Nr4a2 gene in various muscle tissues of Prokr1-rescued mice.
Quad means quadriceps, TA for tibialis anterior, GAS for gastrocnemius, and SOL for soleus muscle tissue. Values indicate mean ± SD (n = 3), **$p < 0.01$, ***$p < 0.001$ vs. AAV-mock control.

Fig. S1

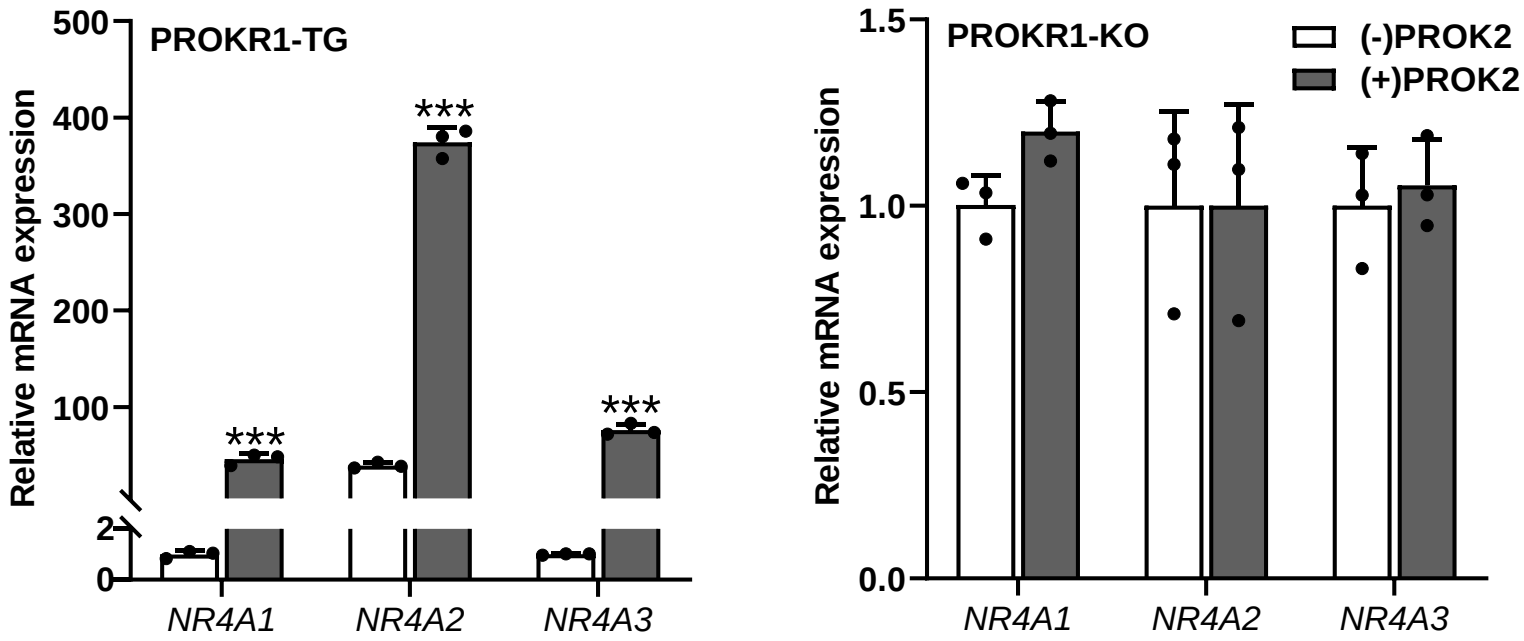
PROKR1-TG
Relative mRNA expression
500
400
300
200
100
2
0
***
***
***
NR4A1
NR4A2
NR4A3
PROKR1-KO
(-)PROK2
(+)PROK2
Relative mRNA expression
1.5
1.0
0.5
0.0
NR4A1
NR4A2
NR4A3

Fig. S2

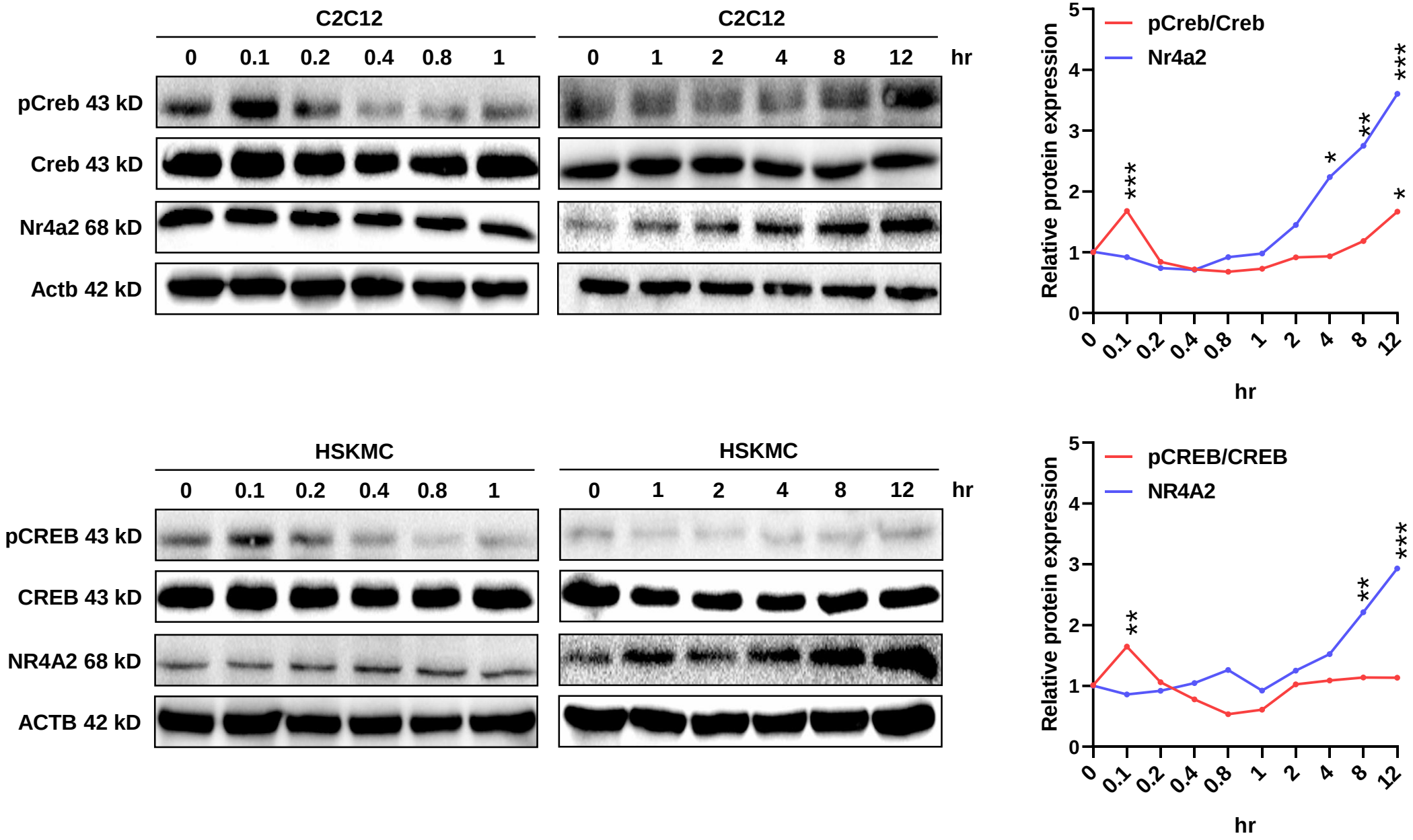
C2C12
0
0.1
0.2
0.4
0.8
1
C2C12
0
1
2
4
8
12
hr
pCreb 43 kD
Creb 43 kD
Nr4a2 68 kD
Actb 42 kD
pCreb/Creb
Nr4a2
Relative protein expression
***
*
**
*
0
1
2
3
4
5
0
0.1
0.2
0.4
0.8
1
2
4
8
12
hr
HSKMC
0
0.1
0.2
0.4
0.8
1
HSKMC
0
1
2
4
8
12
hr
pCREB 43 kD
CREB 43 kD
NR4A2 68 kD
ACTB 42 kD
pCREB/CREB
NR4A2
Relative protein expression
**
**
***
0
1
2
3
4
5
0
0.1
0.2
0.4
0.8
1
2
4
8
12
hr

Fig. S3

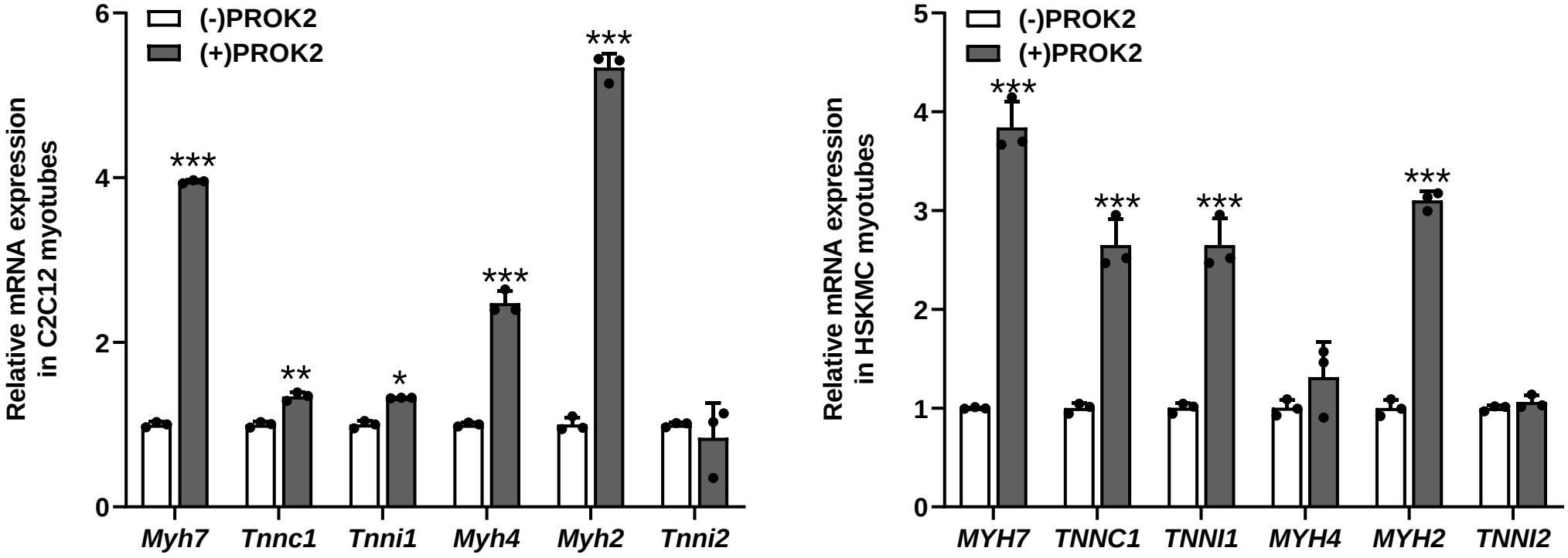
(-)PROK2
(+)PROK2
Relative mRNA expression in C2C12 myotubes
6
4
2
0
***
**
*
***
***
Myh7
Tnnc1
Tnni1
Myh4
Myh2
Tnni2
(-)PROK2
(+)PROK2
Relative mRNA expression in HSKMC myotubes
5
4
3
2
1
0
***
***
***
***
MYH7
TNNC1
TNNI1
MYH4
MYH2
TNNI2

Fig. S4

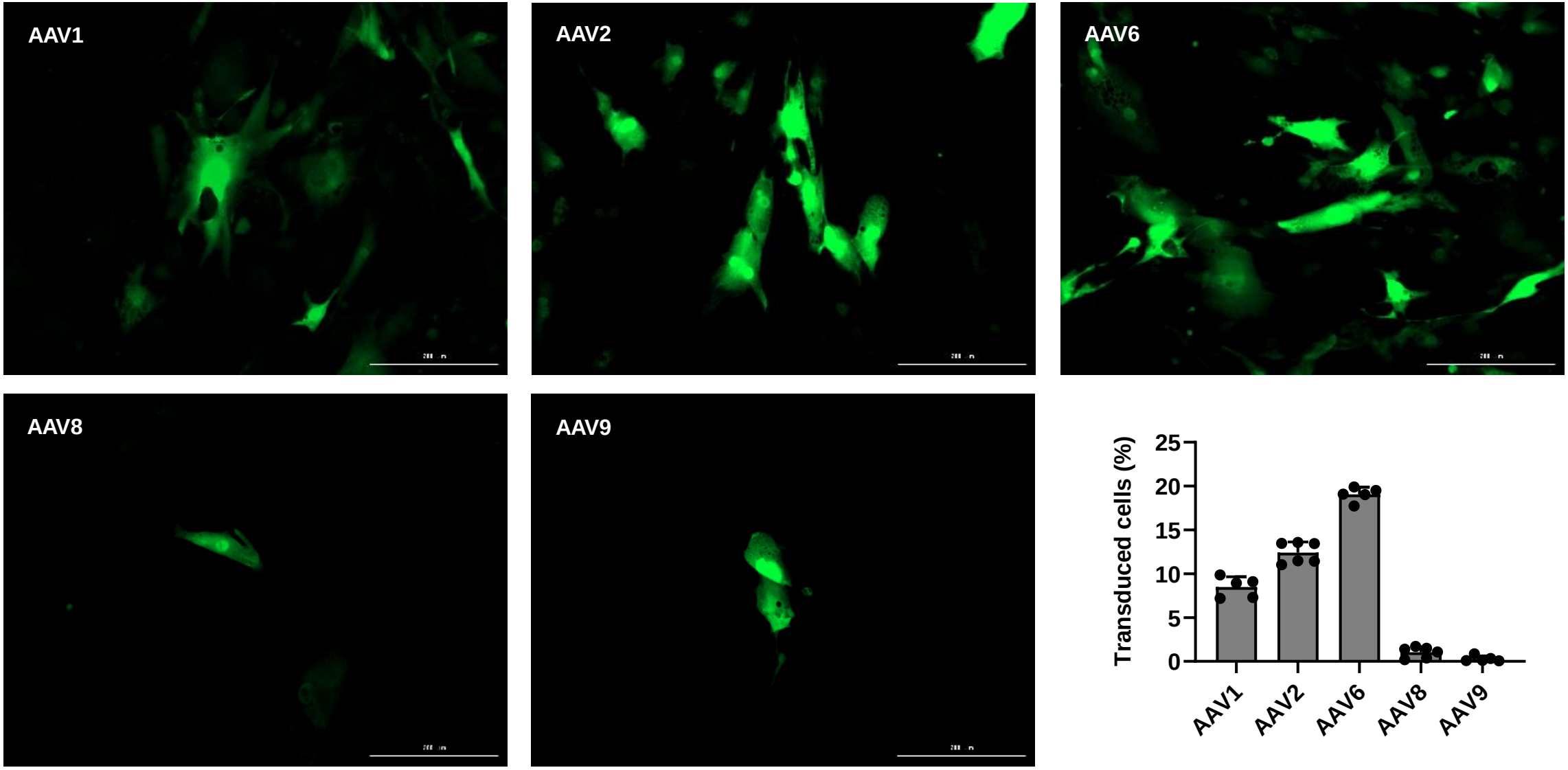
AAV1
AAV2
AAV6
AAV8
AAV9
Transduced cells (%)
25
20
15
10
5
0
AAV1
AAV2
AAV6
AAV8
AAV9

Fig. S5

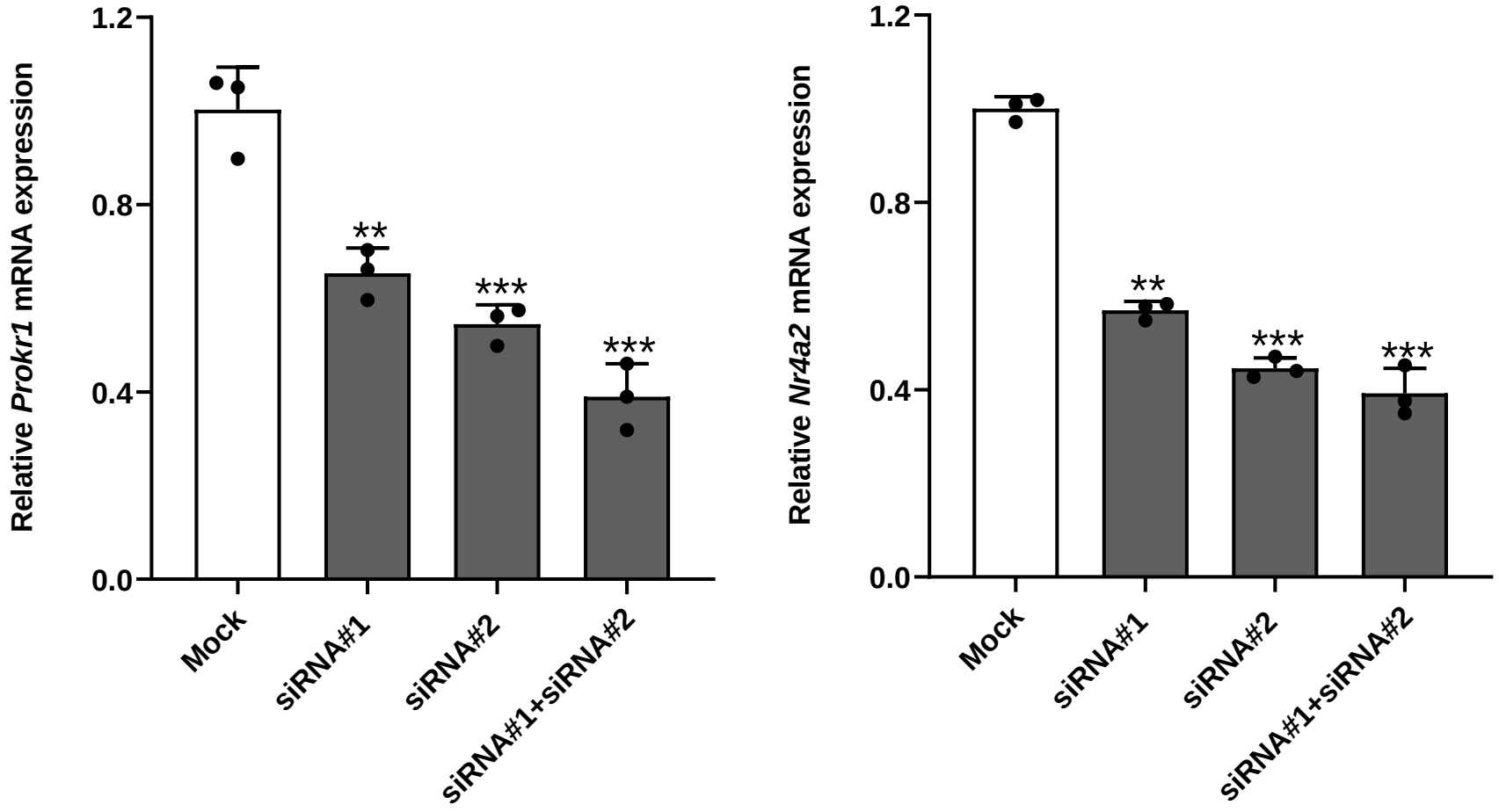
Relative Prokr1 mRNA expression
1.2
0.8
0.4
0.0
**
***
***
Mock
siRNA#1
siRNA#2
siRNA#1+siRNA#2
Relative Nr4a2 mRNA expression
1.2
0.8
0.4
0.0
**
***
***
Mock
siRNA#1
siRNA#2
siRNA#1+siRNA#2

Fig. S6

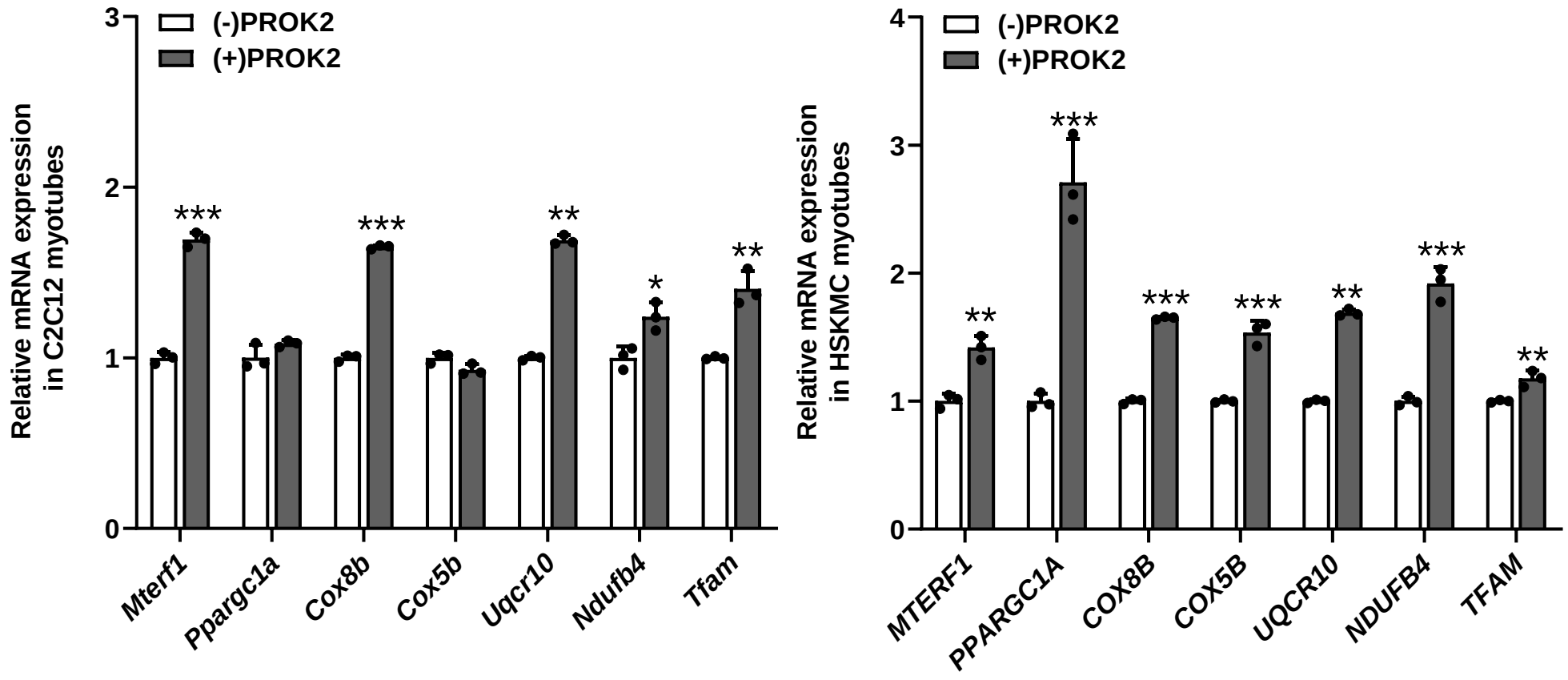
(-)PROK2
(+)PROK2
Relative mRNA expression in C2C12 myotubes
0
1
2
3
***
***
**
*
**
Mterf1
Ppargc1a
Cox8b
Cox5b
Uqcr10
Ndufb4
Tfam
(-)PROK2
(+)PROK2
Relative mRNA expression in HSKMC myotubes
0
1
2
3
4
**
***
***
***
**
***
**
MTERF1
PPARGC1A
COX8B
COX5B
UQCR10
NDUFB4
TFAM

Fig. S7

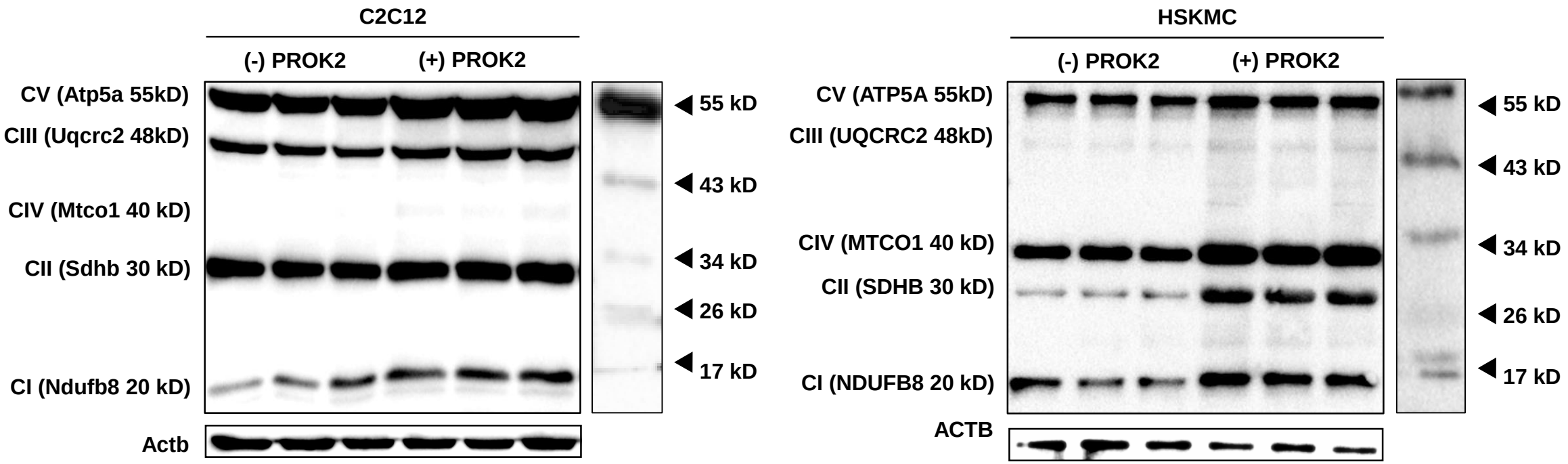
C2C12
(-) PROK2
(+) PROK2
CV (Atp5a 55kD)
CIII (Uqcrc2 48kD)
CIV (Mtco1 40 kD)
CII (Sdhb 30 kD)
CI (Ndufb8 20 kD)
Actb
55 kD
43 kD
34 kD
26 kD
17 kD
HSKMC
(-) PROK2
(+) PROK2
CV (ATP5A 55kD)
CIII (UQCRC2 48kD)
CIV (MTCO1 40 kD)
CII (SDHB 30 kD)
CI (NDUFB8 20 kD)
ACTB
55 kD
43 kD
34 kD
26 kD
17 kD

Fig. S8

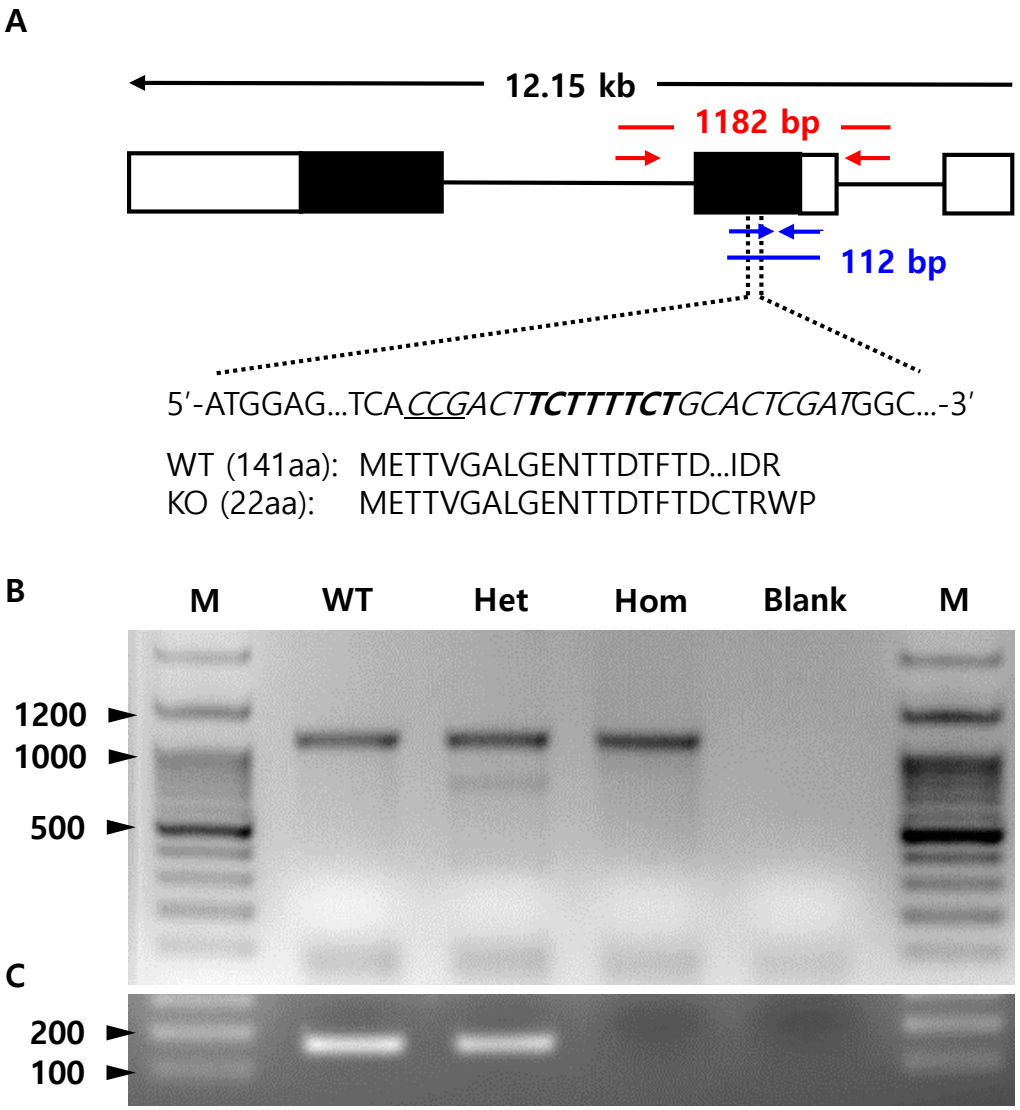
A
12.15 kb
1182 bp
112 bp
5′-ATGGAG...TCACCGACTTCTTTTCTGCACTCGATGGC...-3′
WT (141aa): METTVGALGENTTDTFTD...IDR
KO (22aa): METTVGALGENTTDTFTDCTRWP
B
M
WT
Het
Hom
Blank
M
1200
1000
500
C
200
100

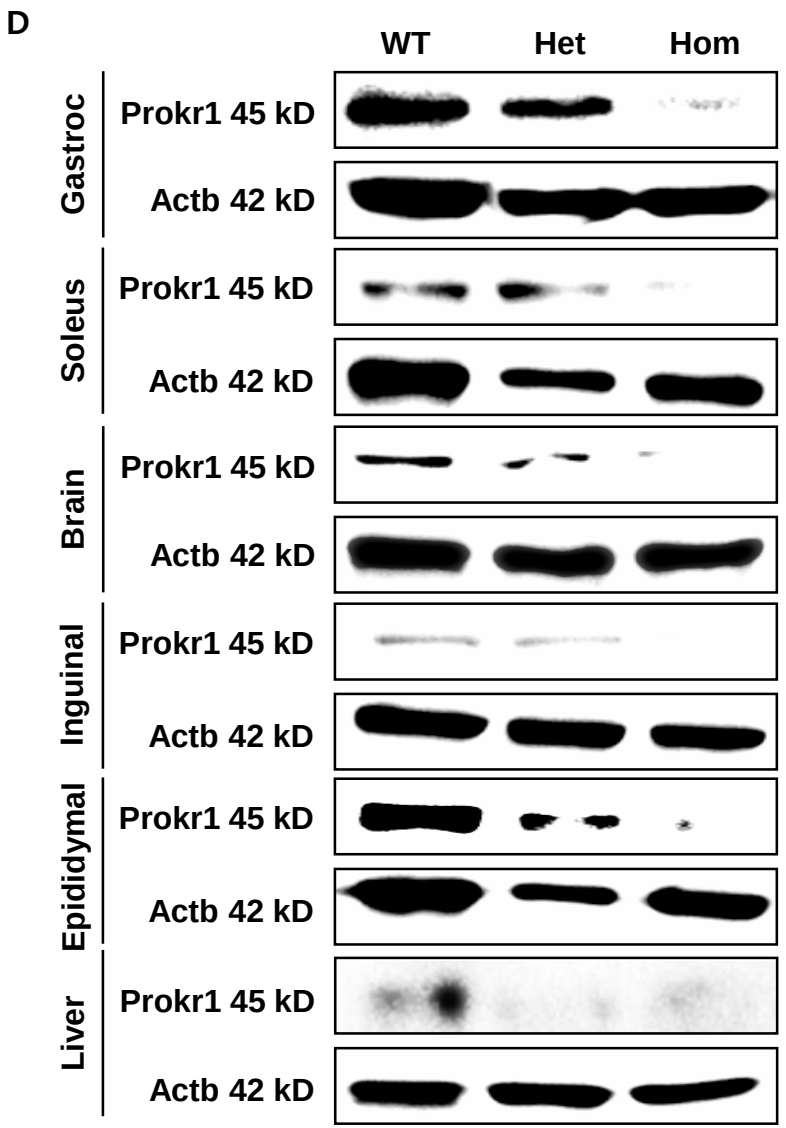
D
WT
Het
Hom
Gastroc
Prokr1 45 kD
Actb 42 kD
Soleus
Prokr1 45 kD
Actb 42 kD
Brain
Prokr1 45 kD
Actb 42 kD
Inguinal
Prokr1 45 kD
Actb 42 kD
Epididymal
Prokr1 45 kD
Actb 42 kD
Liver
Prokr1 45 kD
Actb 42 kD

Fig. S9

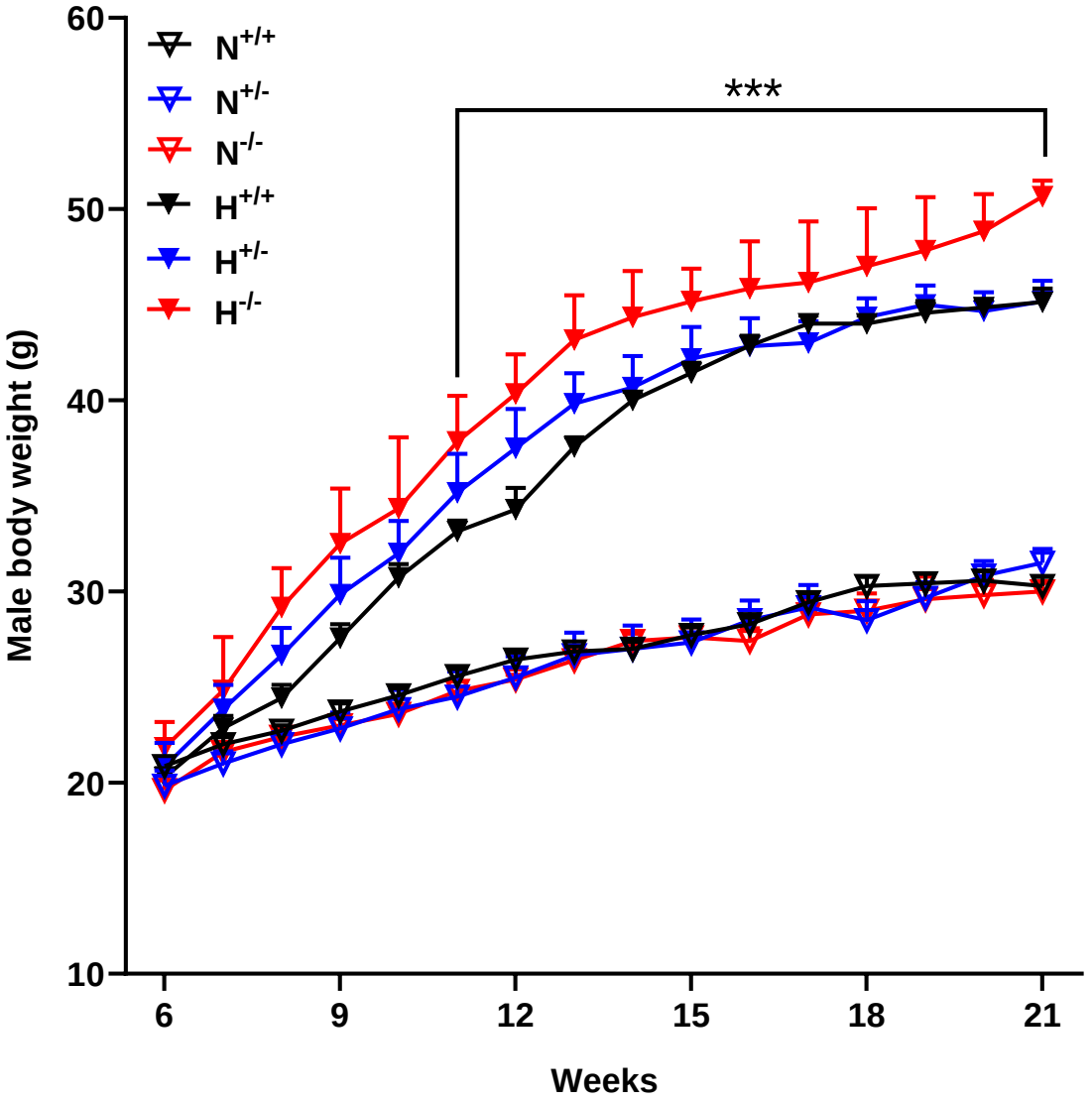
60
50
40
30
20
10
Male body weight (g)
N+/+
N+/-
N-/-
H+/+
H+/-
H-/-
***
6
9
12
15
18
21
Weeks

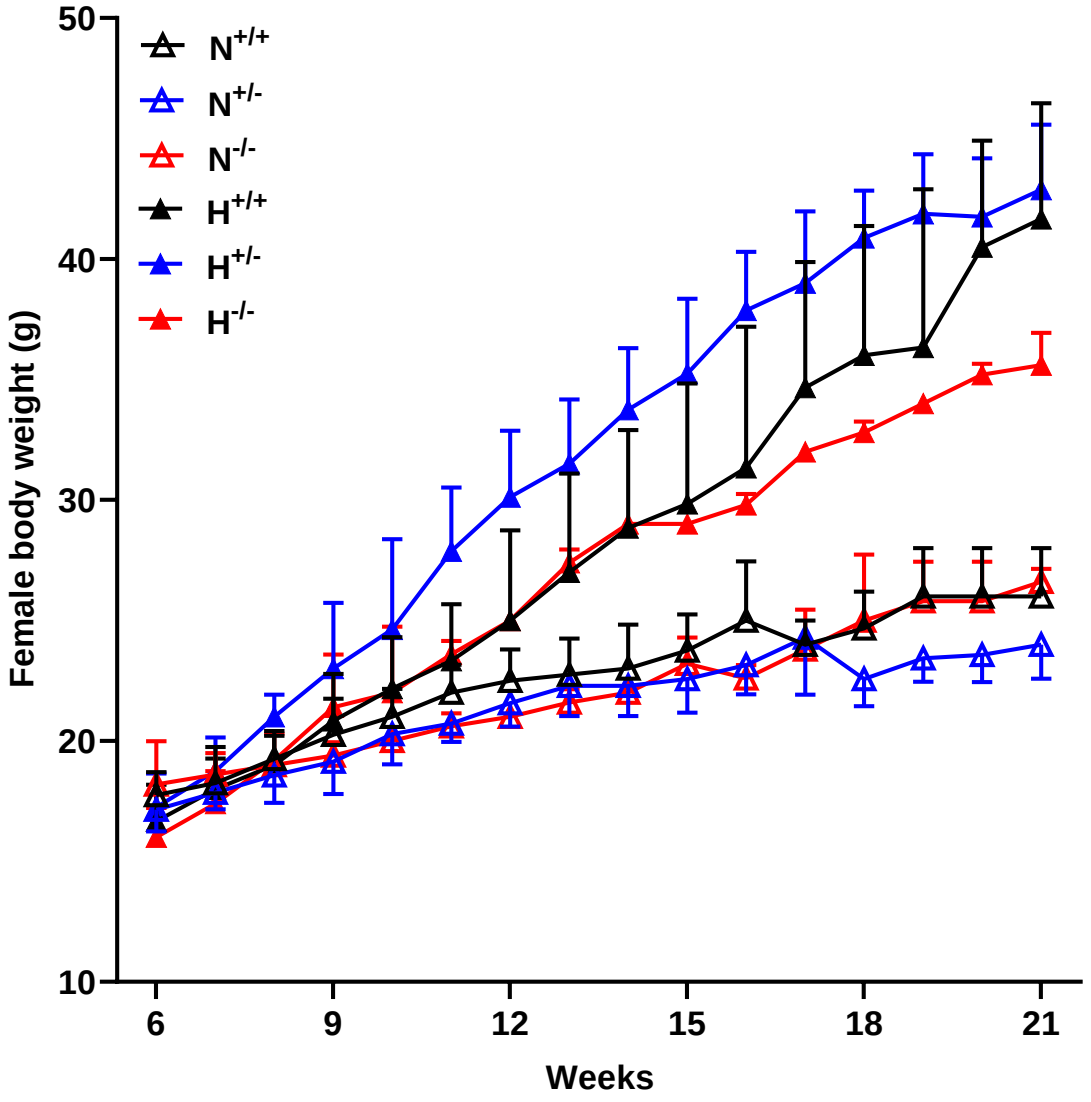
50
40
30
20
10
Female body weight (g)
N+/+
N+/-
N-/-
H+/+
H+/-
H-/-
6
9
12
15
18
21
Weeks

Fig. S10

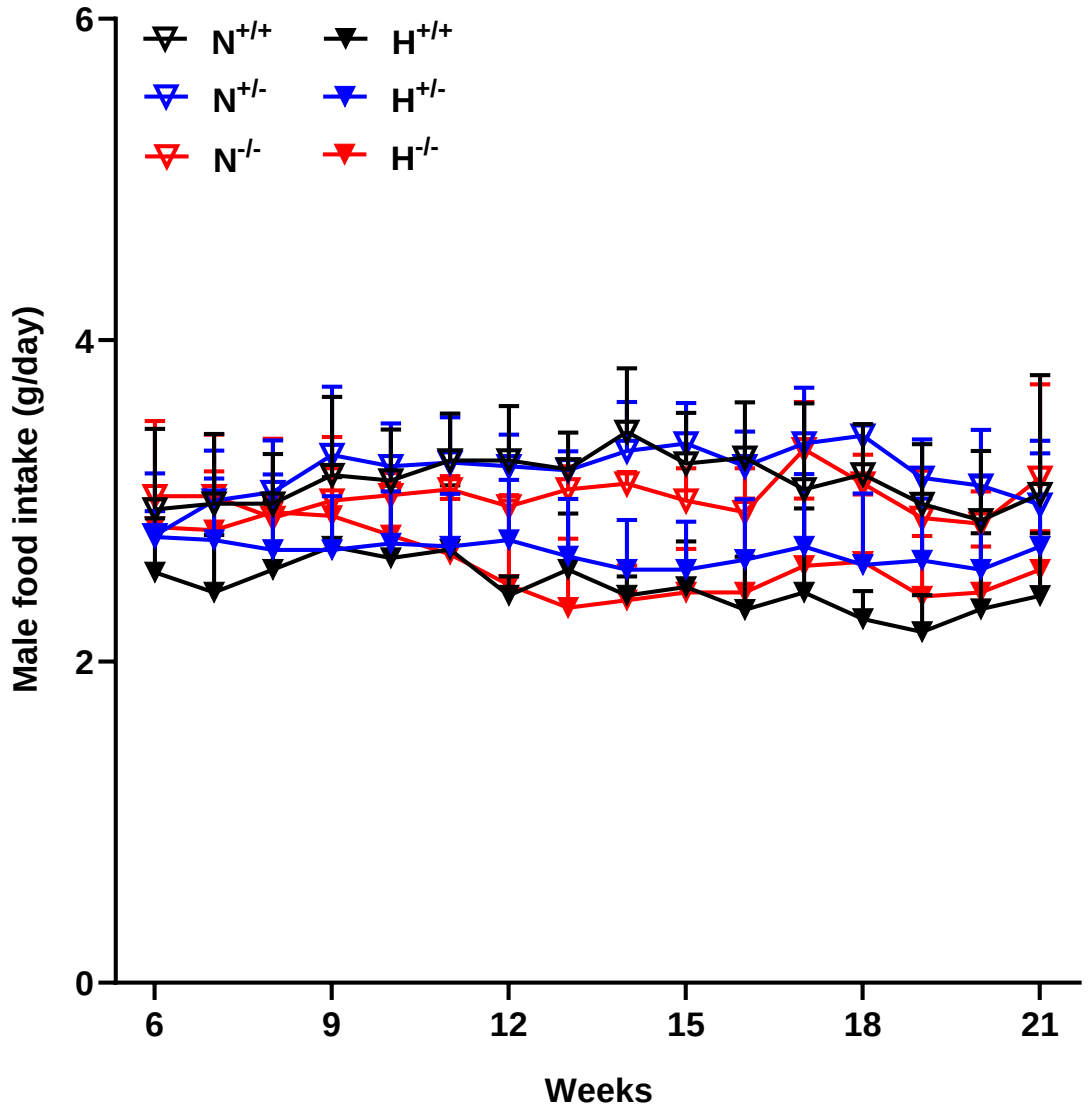
N+/+
H+/+
N+/-
H+/-
N-/-
H-/-
Male food intake (g/day)
0
2
4
6
6
9
12
15
18
21
Weeks

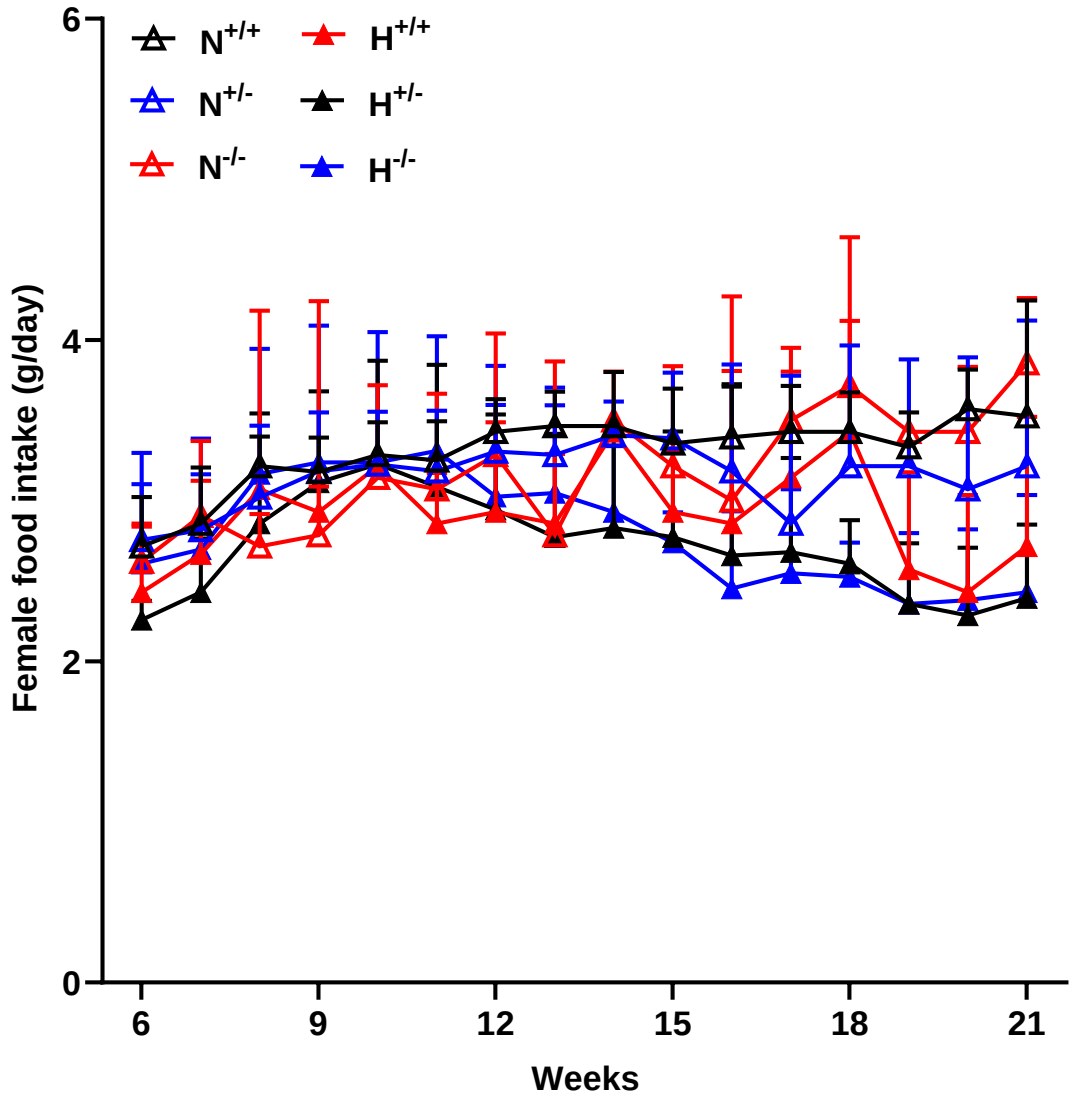
N+/+
H+/+
N+/-
H+/-
N-/-
H-/-
Female food intake (g/day)
0
2
4
6
6
9
12
15
18
21
Weeks

Fig. S11

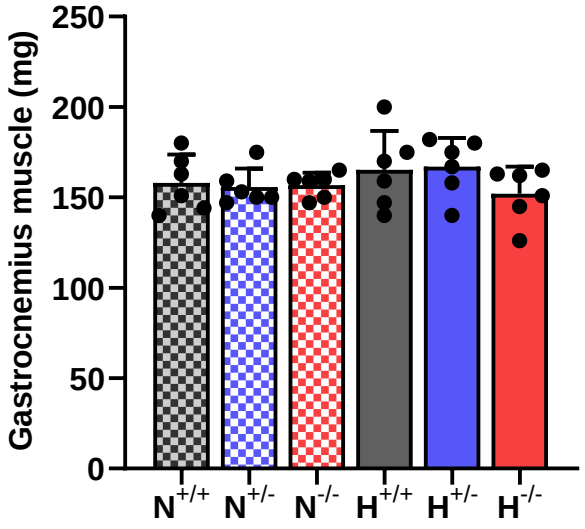
Gastrocnemius muscle (mg)
250
200
150
100
50
0
N+/+ N+/- N-/- H+/+ H+/- H-/-

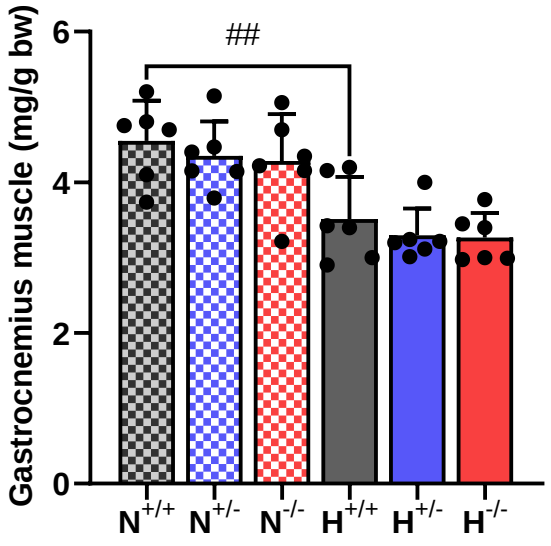
Gastrocnemius muscle (mg/g bw)
6
4
2
0
##
N+/+ N+/- N-/- H+/+ H+/- H-/-

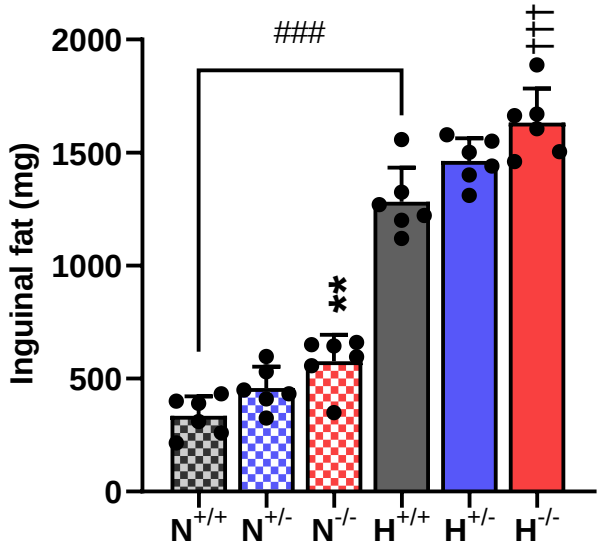
Inguinal fat (mg)
2000
1500
1000
500
0
###
**
†††
N+/+ N+/- N-/- H+/+ H+/- H-/-

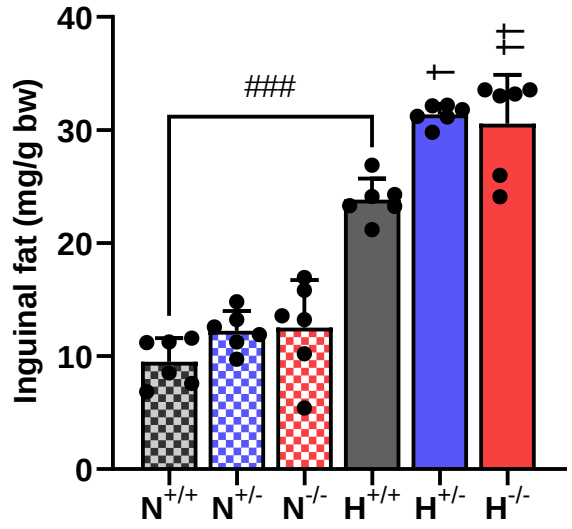
Inguinal fat (mg/g bw)
40
30
20
10
0
###
†
††
N+/+ N+/- N-/- H+/+ H+/- H-/-

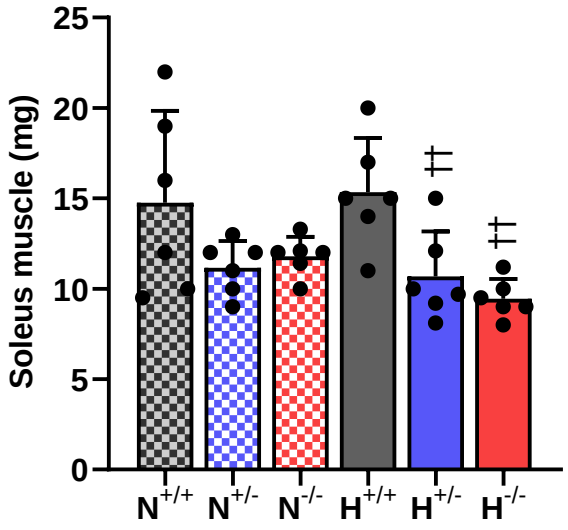
Soleus muscle (mg)
25
20
15
10
5
0
††
††
N+/+ N+/- N-/- H+/+ H+/- H-/-

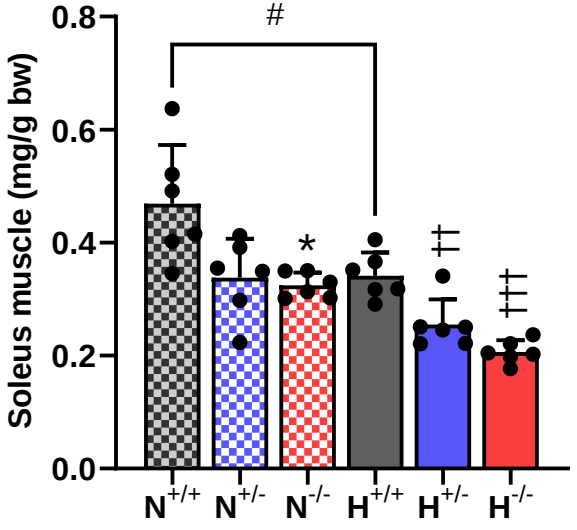
Soleus muscle (mg/g bw)
0.8
0.6
0.4
0.2
0.0
#
*
††
†††
N+/+ N+/- N-/- H+/+ H+/- H-/-

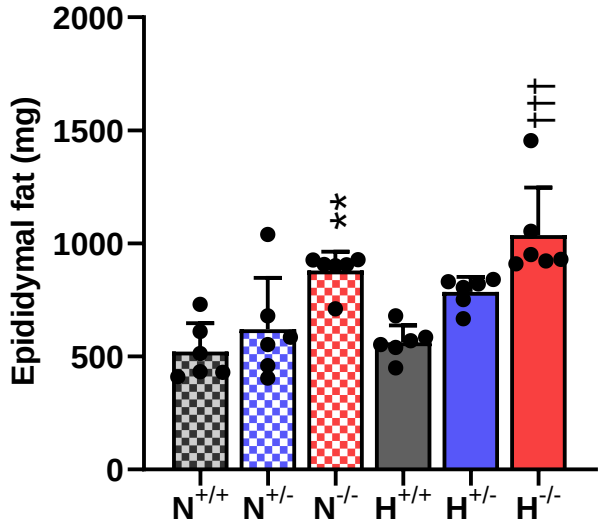
Epididymal fat (mg)
2000
1500
1000
500
0
**
†††
N+/+ N+/- N-/- H+/+ H+/- H-/-

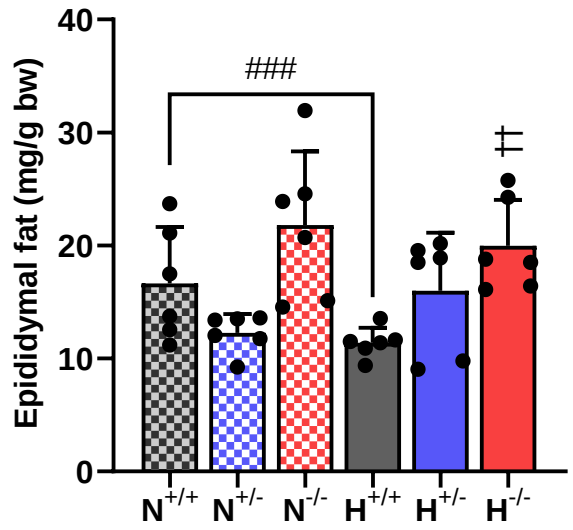
Epididymal fat (mg/g bw)
40
30
20
10
0
###
††
N+/+ N+/- N-/- H+/+ H+/- H-/-

Fig. S12

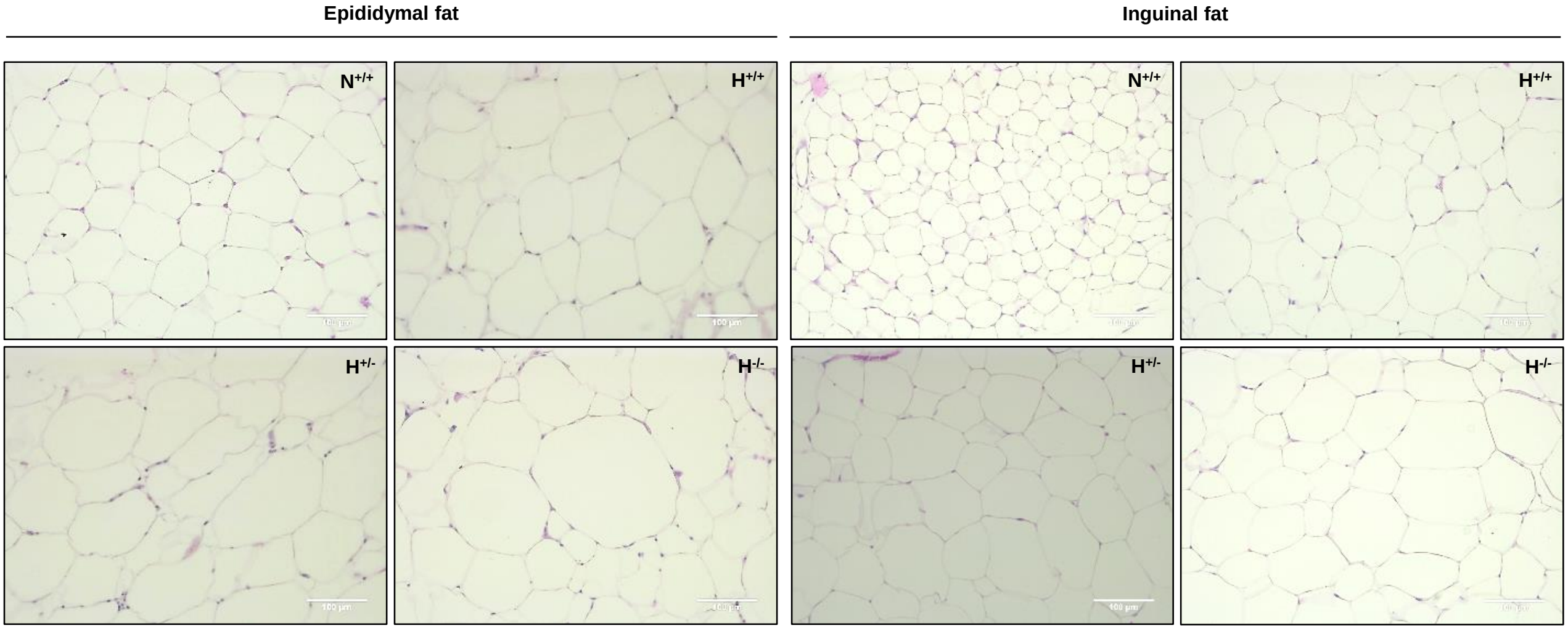

Fig. S13

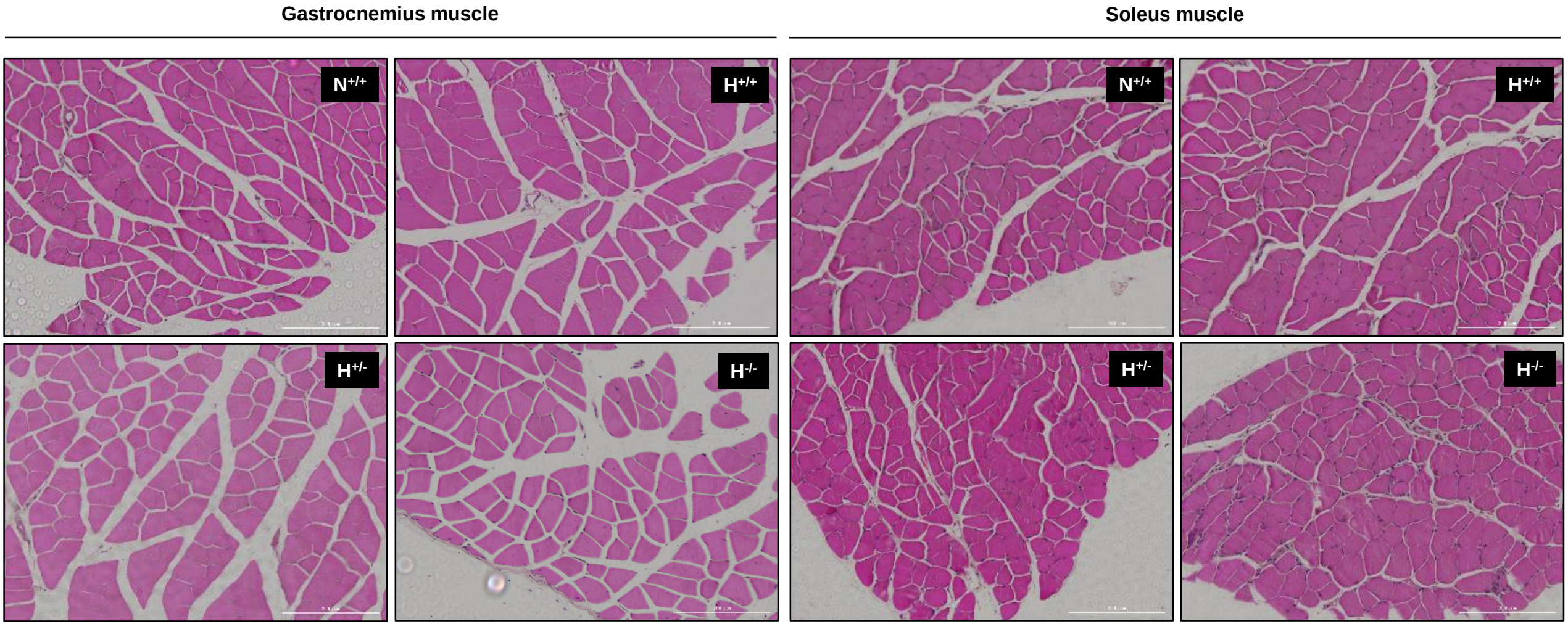

Fig. S14

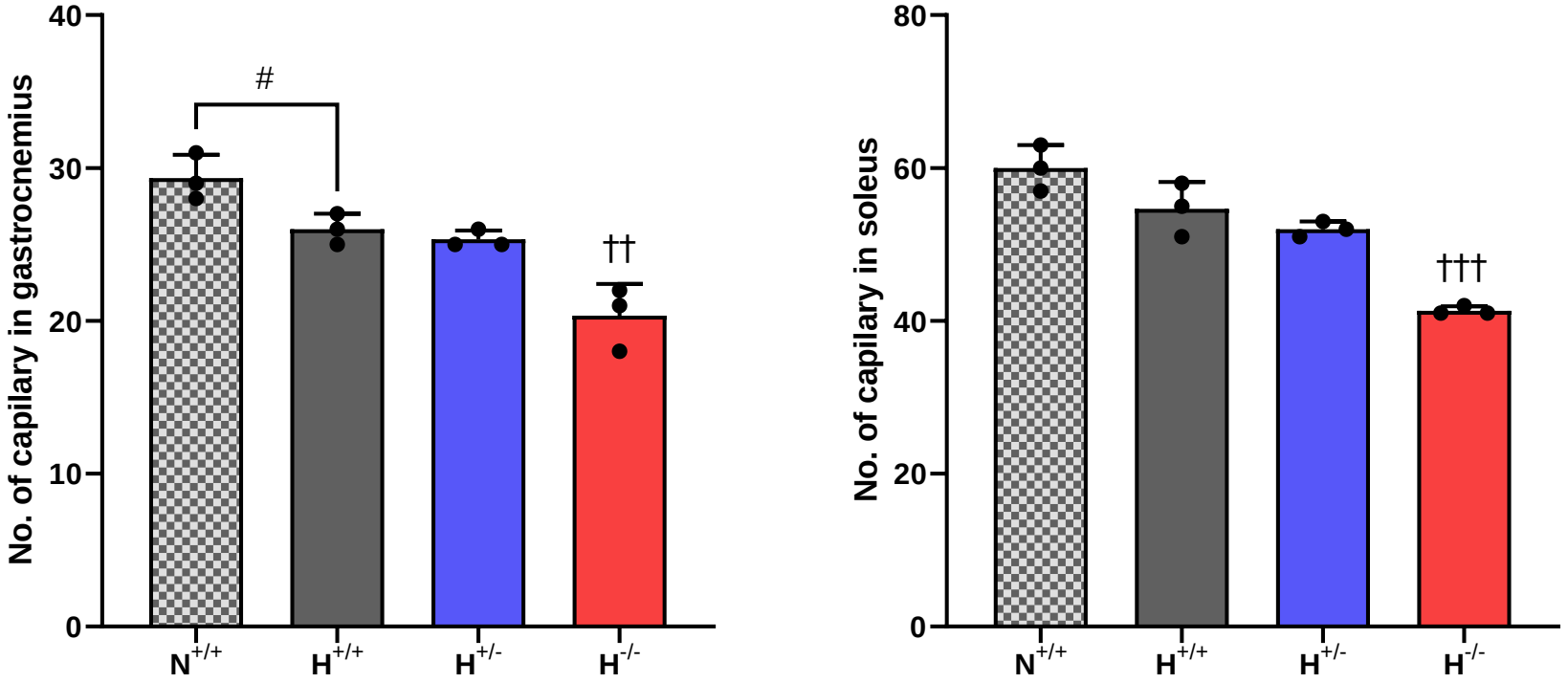
No. of capilary in gastrocnemius
40
30
20
10
0
#
††
N+/+
H+/+
H+/-
H-/-
No. of capilary in soleus
80
60
40
20
0
†††
N+/+
H+/+
H+/-
H-/-

Fig. S15

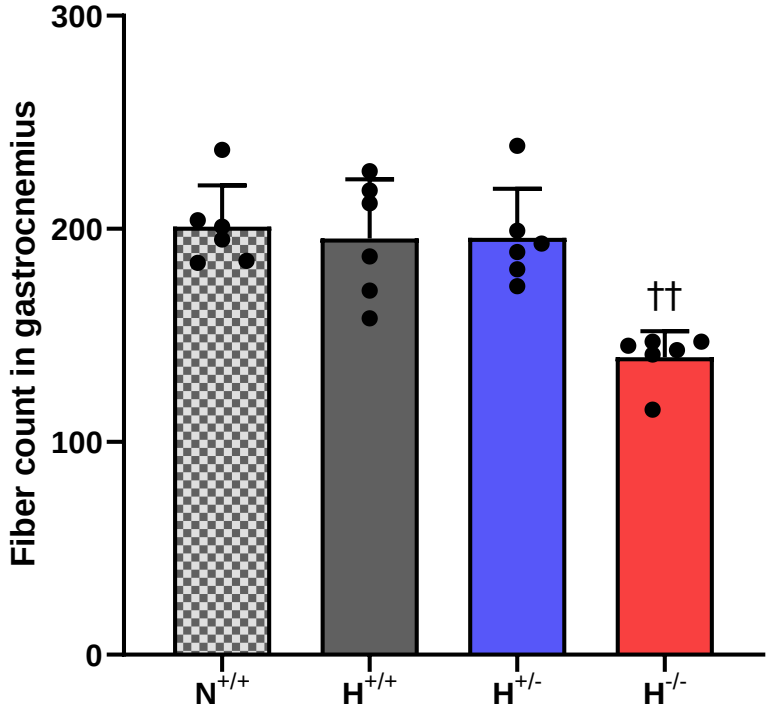
Fiber count in gastrocnemius
300
200
100
0
††
N+/+
H+/+
H+/-
H-/-

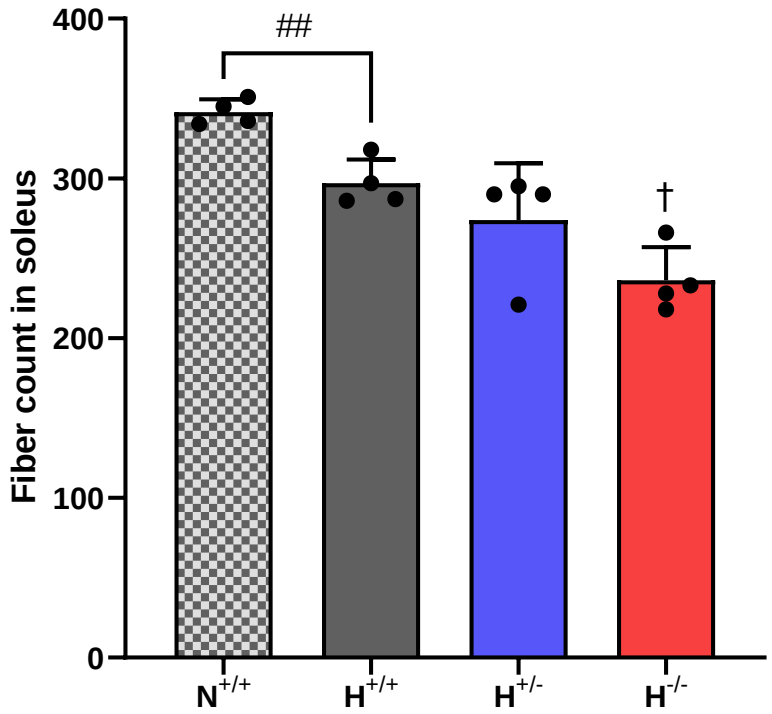
Fiber count in soleus
400
300
200
100
0
##
†
N+/+
H+/+
H+/-
H-/-

Fig. S16

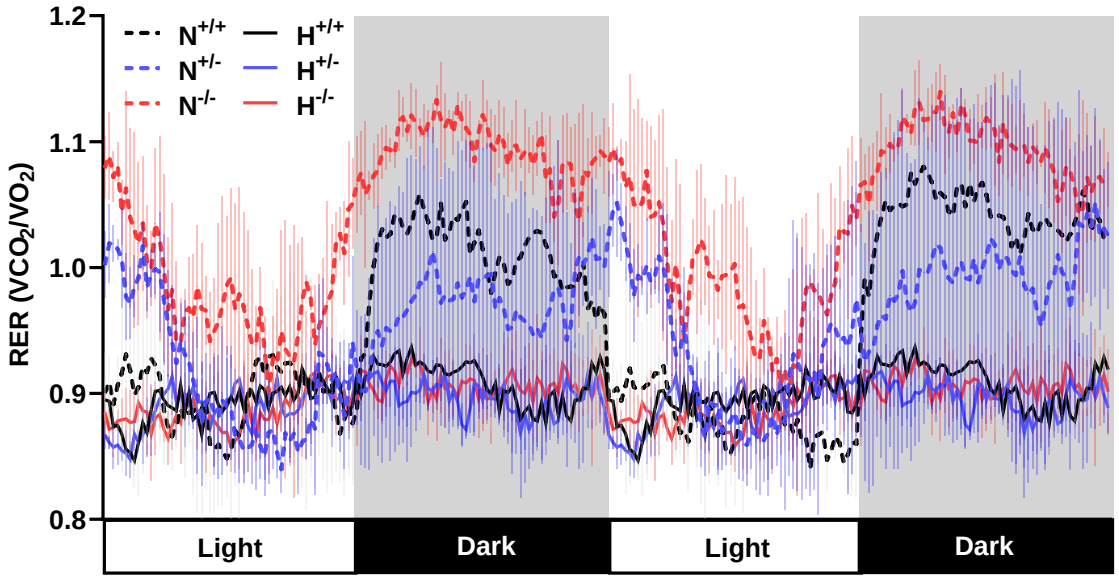
1.2
1.1
1.0
0.9
0.8
RER (VCO2/VO2)
N+/+
H+/+
N+/-
H+/-
N-/-
H-/-
Light
Dark
Light
Dark

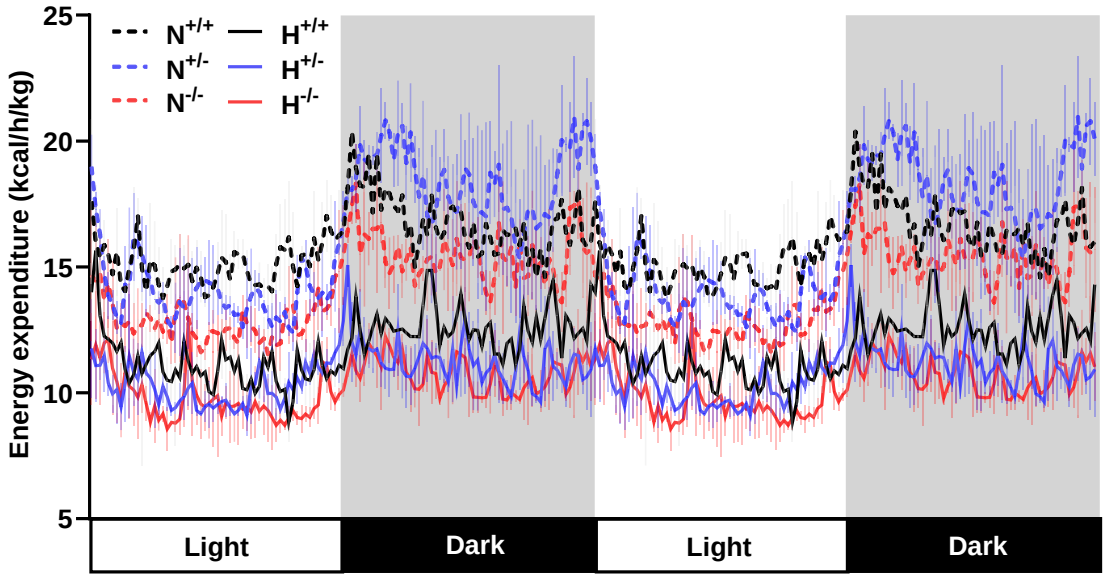
25
20
15
10
5
Energy expenditure (kcal/h/kg)
N+/+
H+/+
N+/-
H+/-
N-/-
H-/-
Light
Dark
Light
Dark

Fig. S17

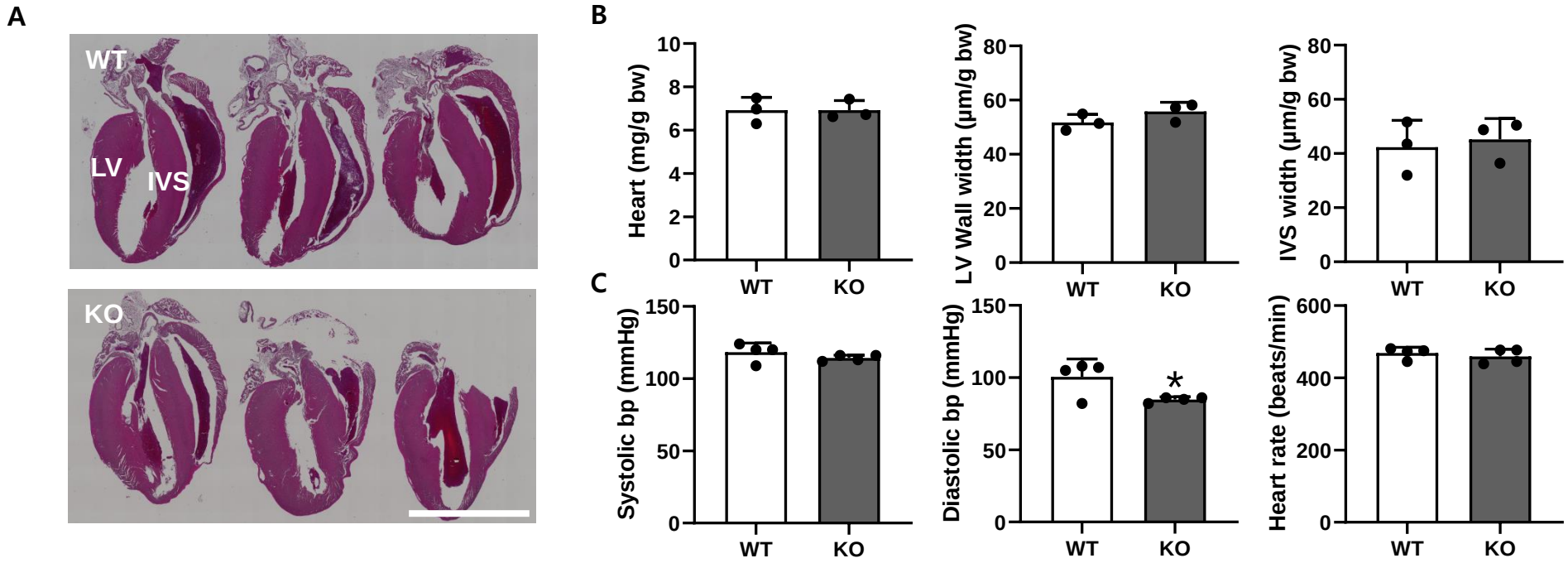
A
WT
LV
IVS
KO
B
Heart (mg/g bw)
LV Wall width (μm/g bw)
IVS width (μm/g bw)
C
Systolic bp (mmHg)
Diastolic bp (mmHg)
Heart rate (beats/min)
WT
KO
*

Fig. S18

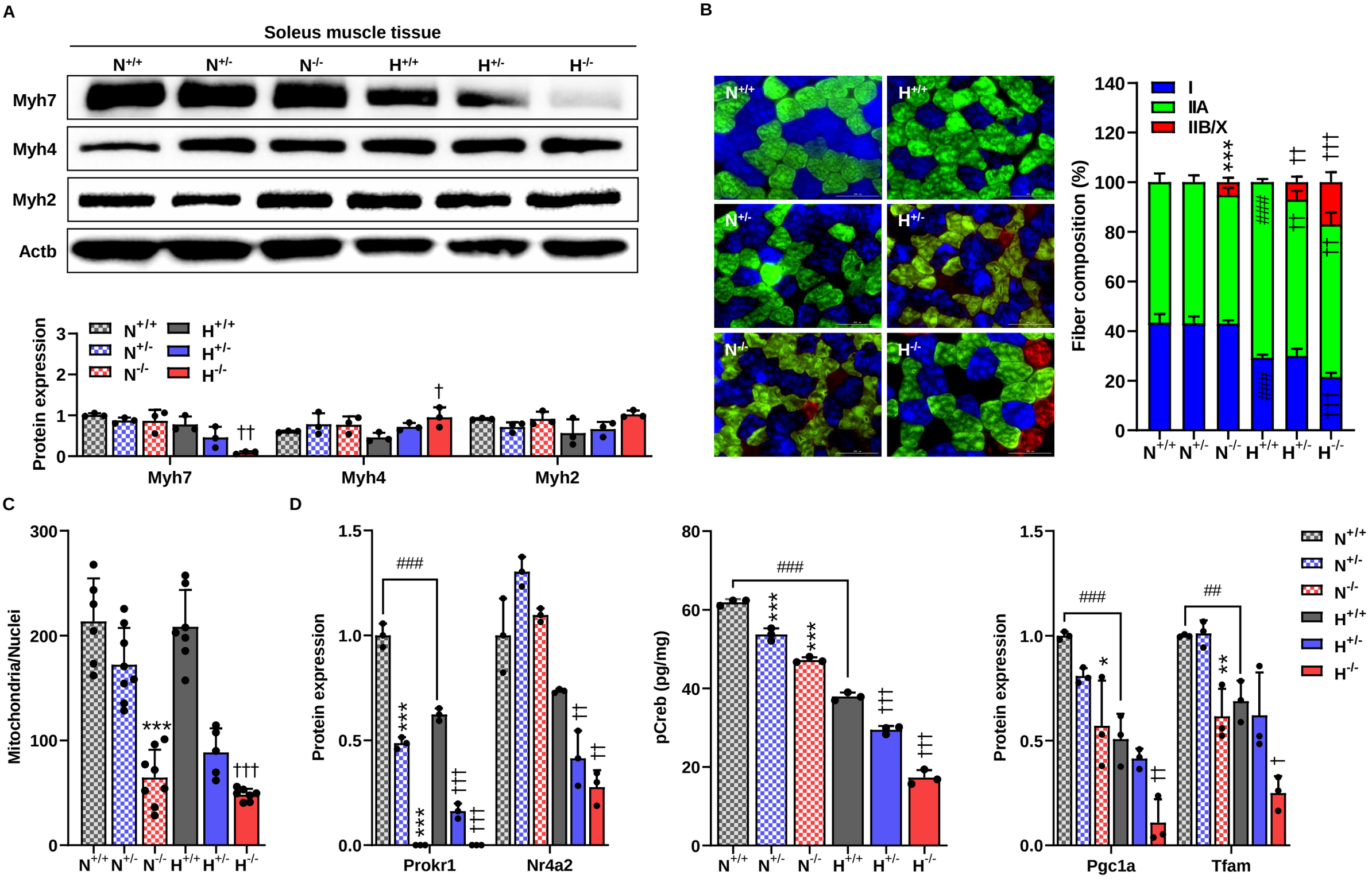
A
Soleus muscle tissue
N+/+
N+/-
N-/-
H+/+
H+/-
H-/-
Myh7
Myh4
Myh2
Actb
Protein expression
Myh7
Myh4
Myh2
B
Fiber composition (%)
I
IIA
IIB/X
C
Mitochondria/Nuclei
D
Protein expression
Prokr1
Nr4a2
pCreb (pg/mg)
Protein expression
Pgc1a
Tfam

Fig. S19

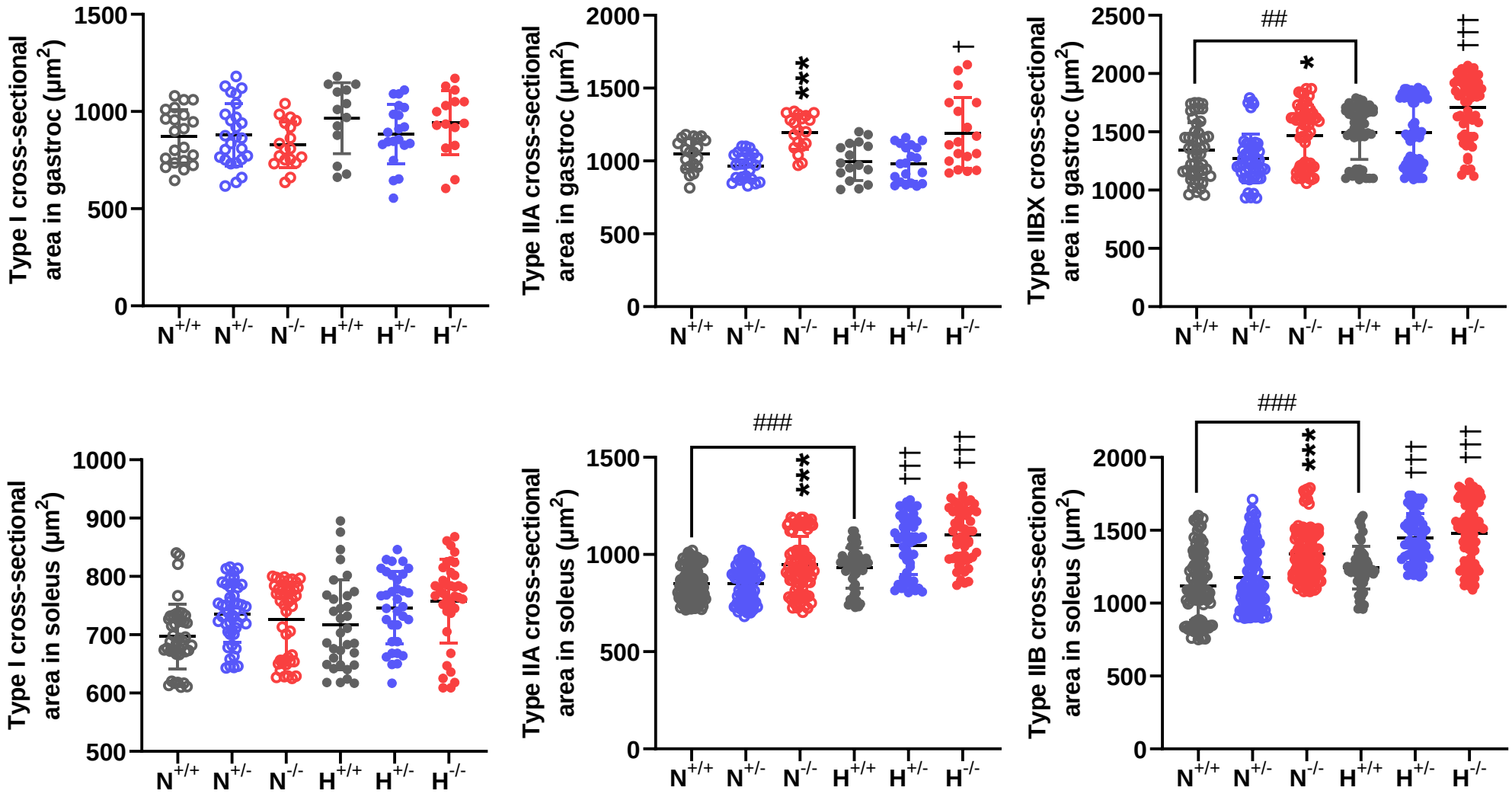
Type I cross-sectional area in gastroc (μm²)
1500
1000
500
0
N+/+ N+/- N-/- H+/+ H+/- H-/-
Type IIA cross-sectional area in gastroc (μm²)
2000
1500
1000
500
0
***
†
Type IIBX cross-sectional area in gastroc (μm²)
2500
2000
1500
1000
500
0
##
*
†††
Type I cross-sectional area in soleus (μm²)
1000
900
800
700
600
500
Type IIA cross-sectional area in soleus (μm²)
1500
1000
500
0
###
***
†††
Type IIB cross-sectional area in soleus (μm²)
2000
1500
1000
500
0
###
***
†††

Fig. S20

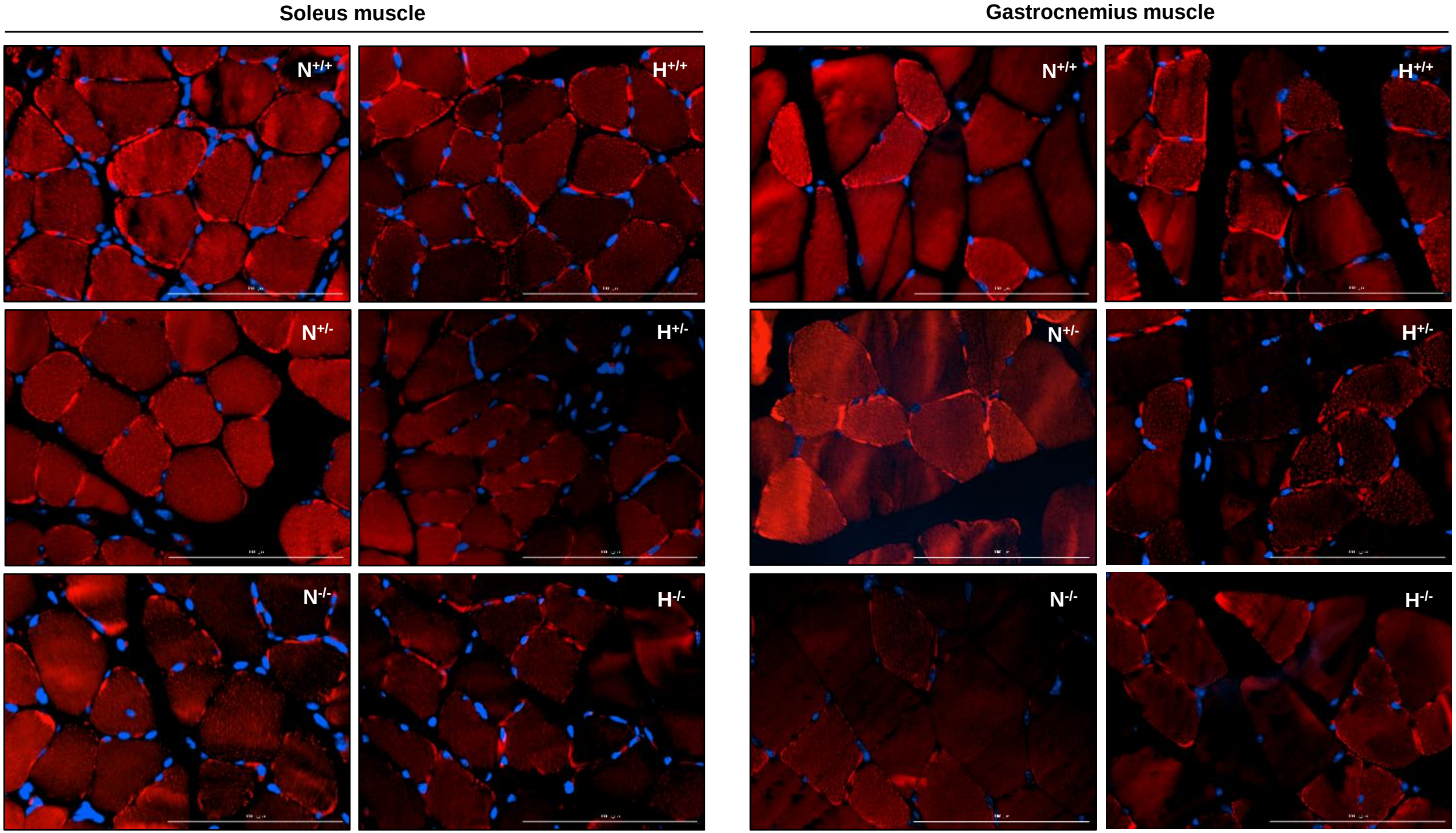

Fig. S21

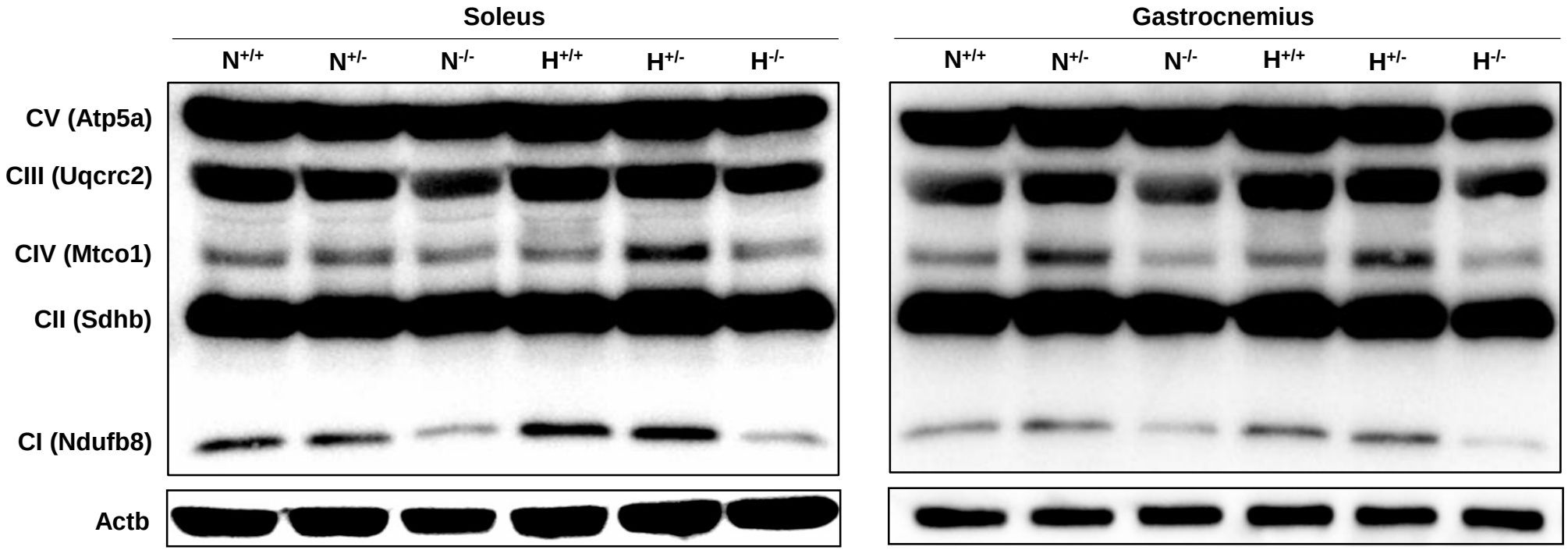
Soleus
Gastrocnemius
N+/+
N+/-
N-/-
H+/+
H+/-
H-/-
CV (Atp5a)
CIII (Uqcrc2)
CIV (Mtco1)
CII (Sdhb)
CI (Ndufb8)
Actb

Fig. S22

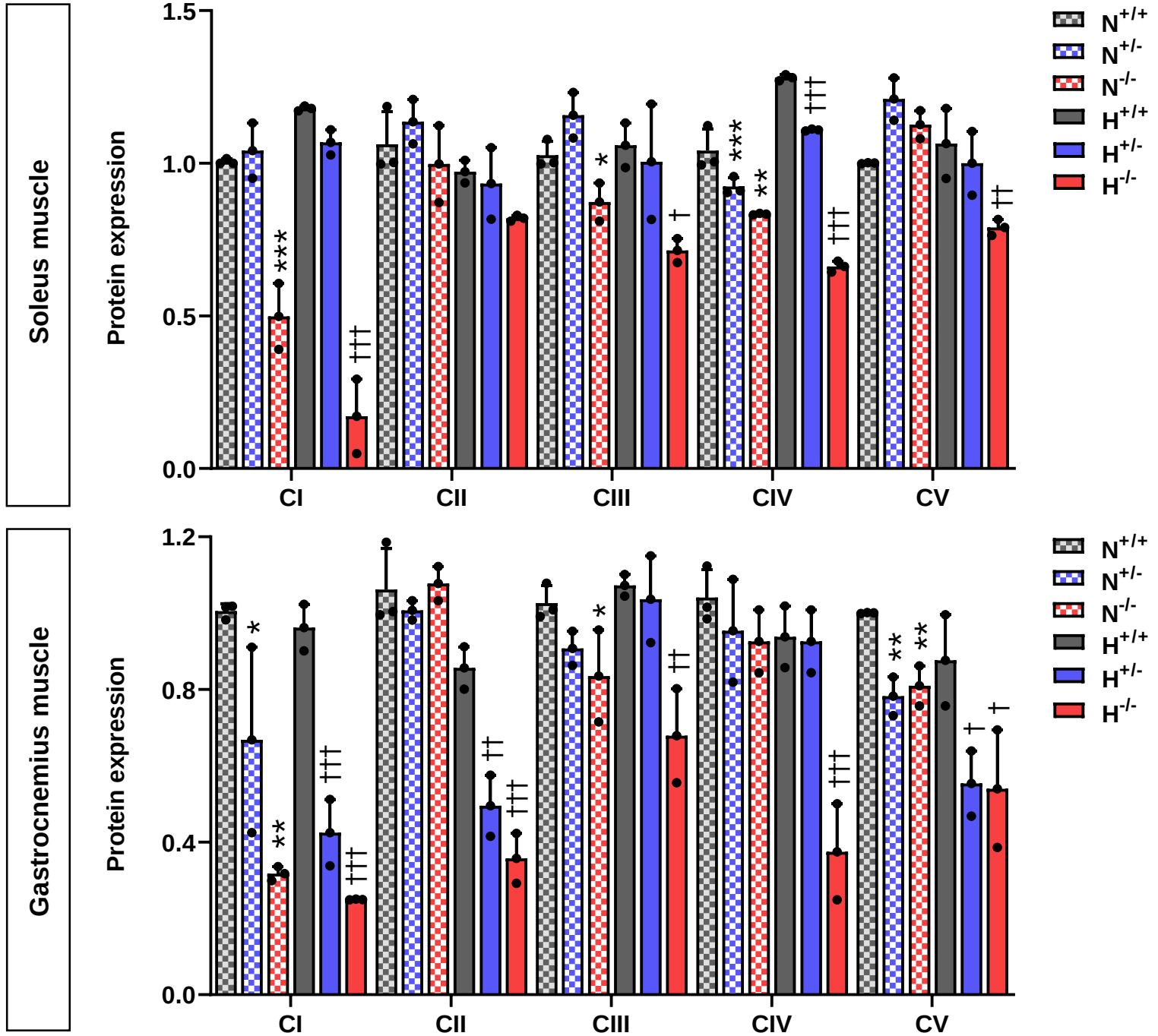
Soleus muscle
Protein expression
1.5
1.0
0.5
0.0
CI
CII
CIII
CIV
CV
N+/+
N+/-
N-/-
H+/+
H+/-
H-/-
Gastrocnemius muscle
Protein expression
1.2
0.8
0.4
0.0
CI
CII
CIII
CIV
CV
N+/+
N+/-
N-/-
H+/+
H+/-
H-/-

Fig. S23

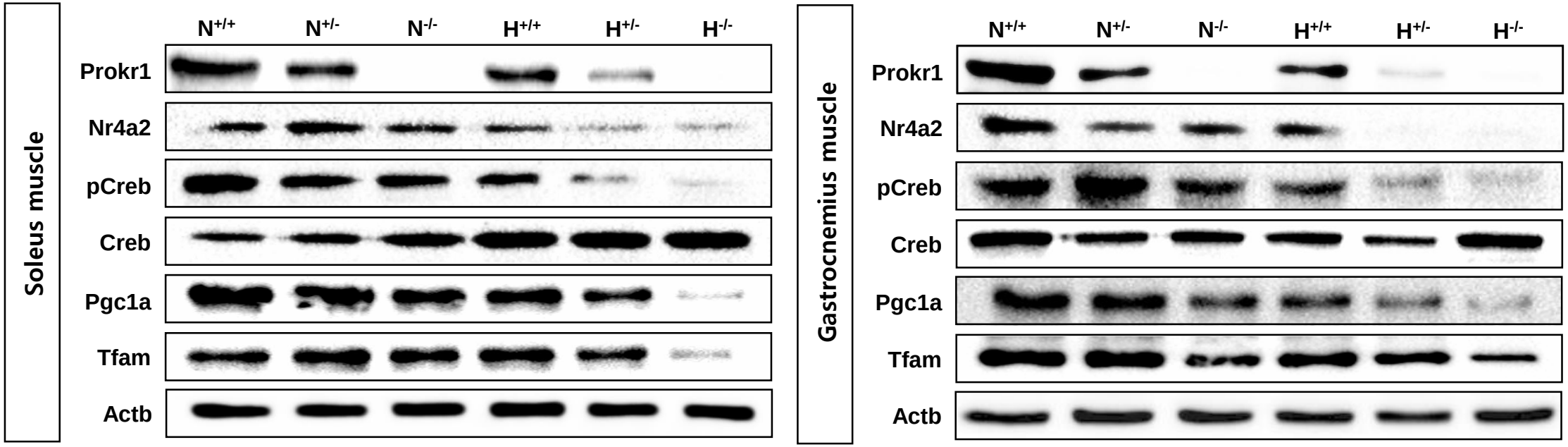
Soleus muscle
N+/+
N+/-
N-/-
H+/+
H+/-
H-/-
Prokr1
Nr4a2
pCreb
Creb
Pgc1a
Tfam
Actb
Gastrocnemius muscle
N+/+
N+/-
N-/-
H+/+
H+/-
H-/-
Prokr1
Nr4a2
pCreb
Creb
Pgc1a
Tfam
Actb

Fig. S24

Quadriceps

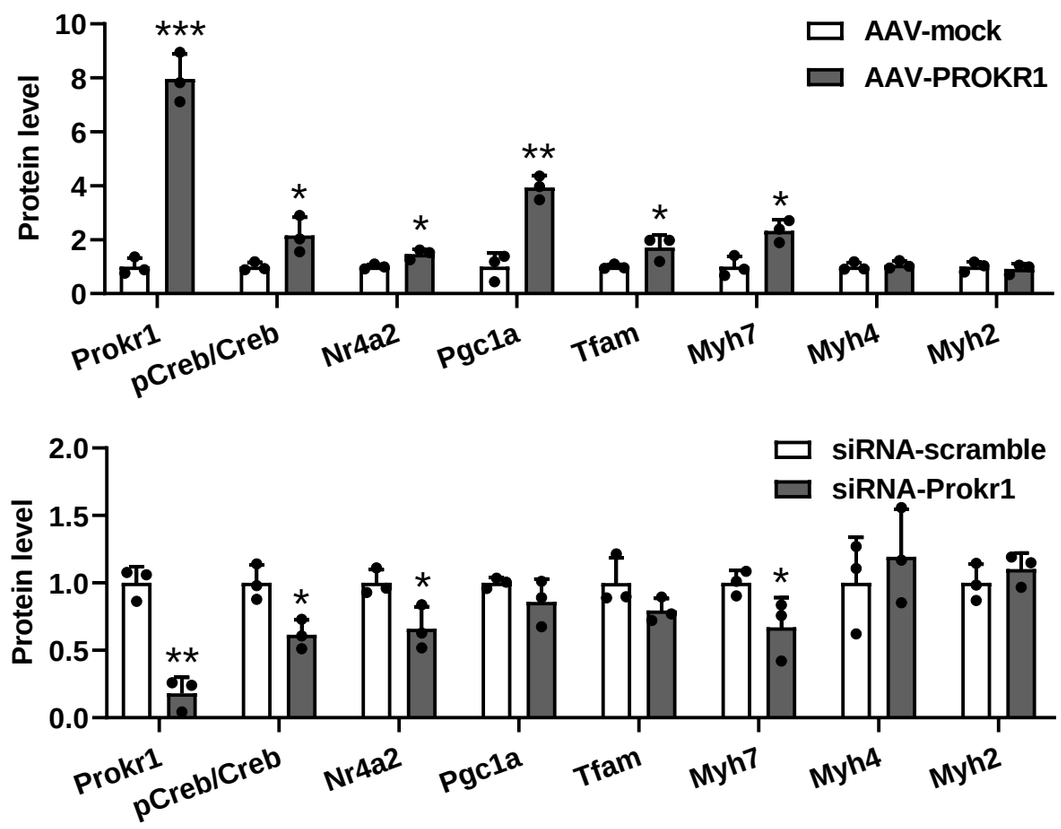

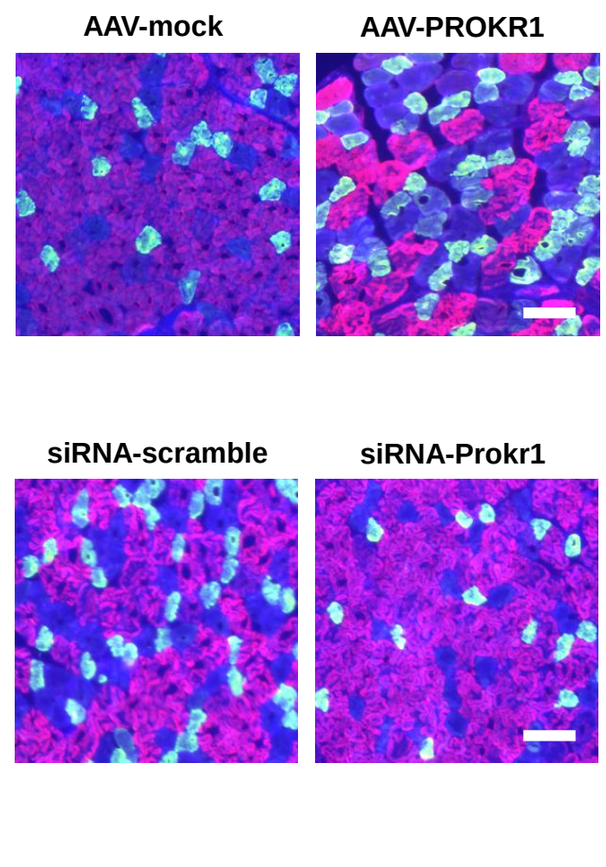

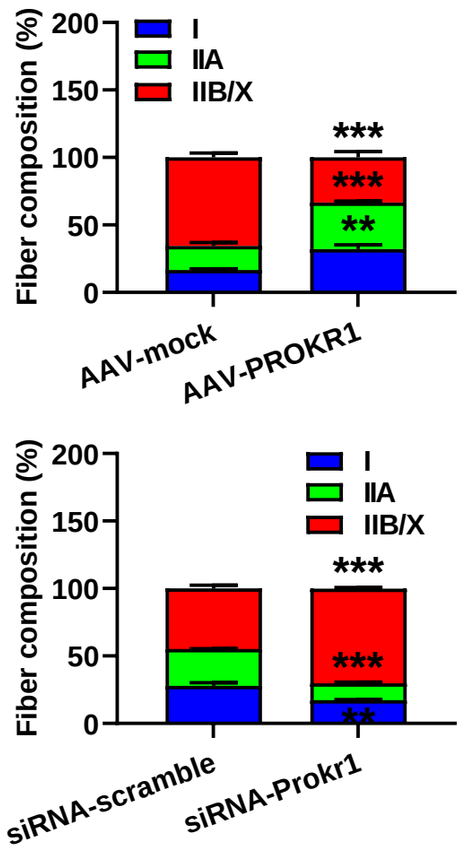

Tibialis anterior

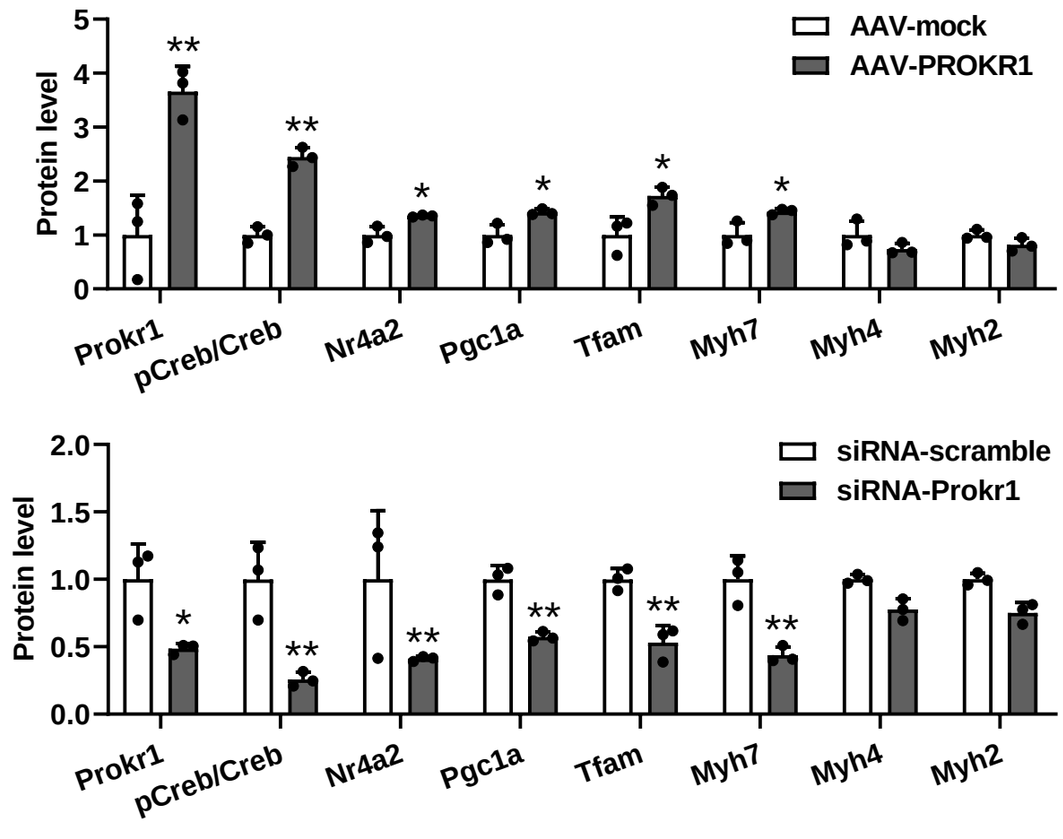

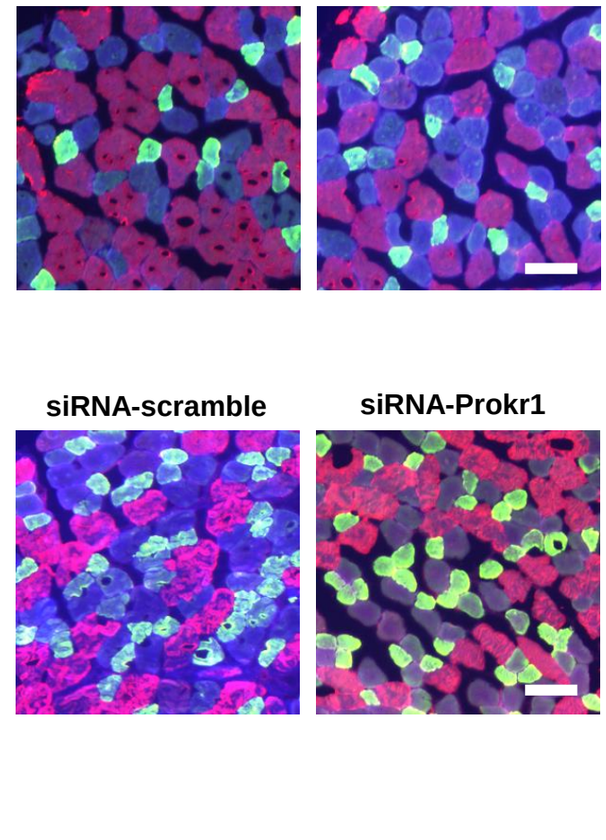

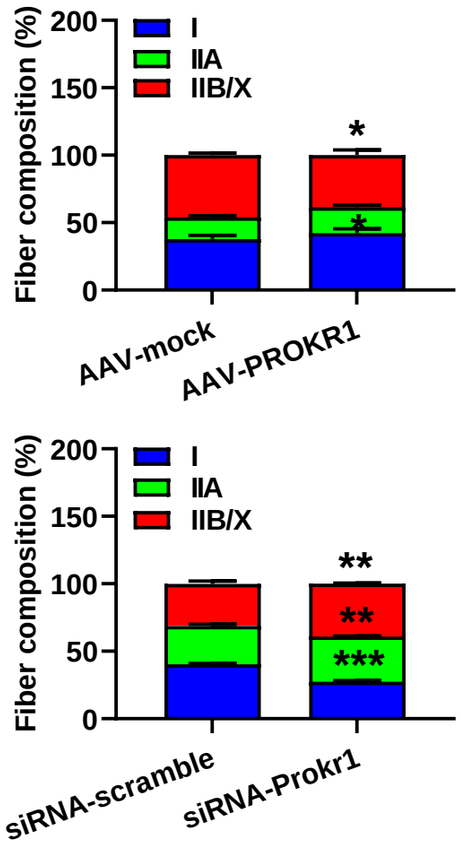

Soleus

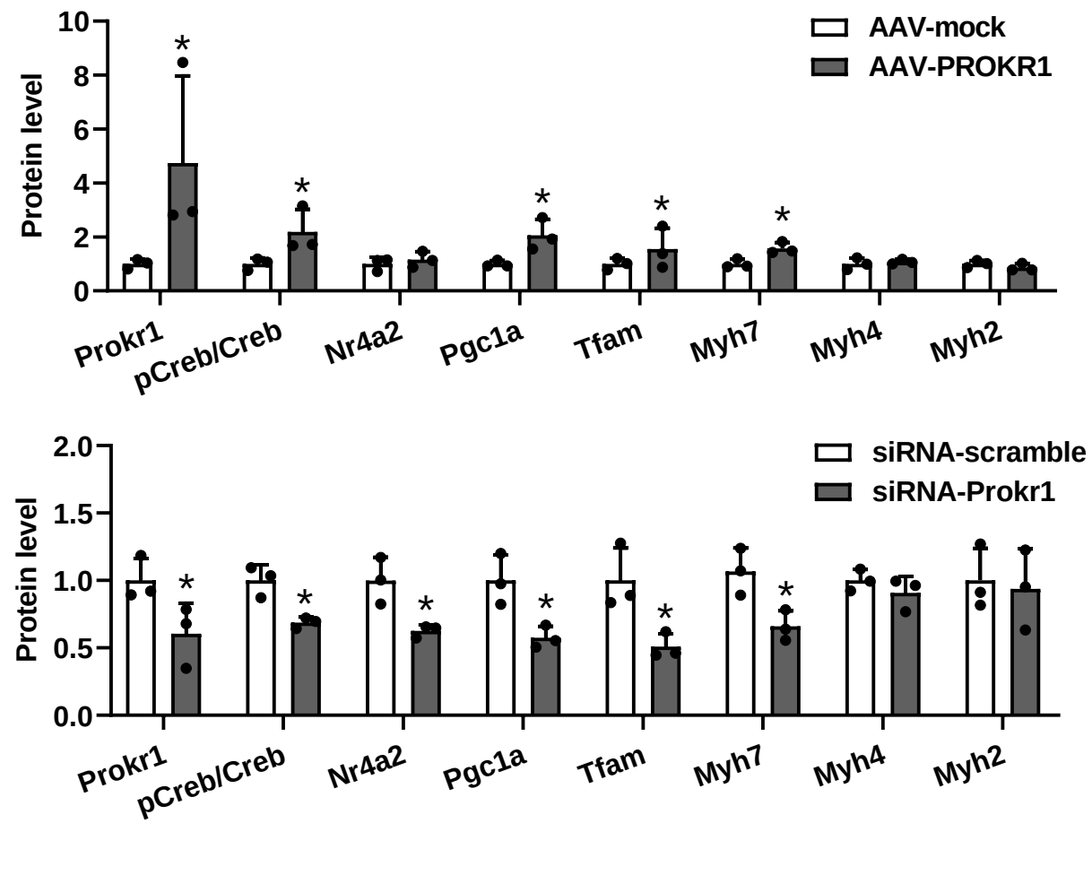

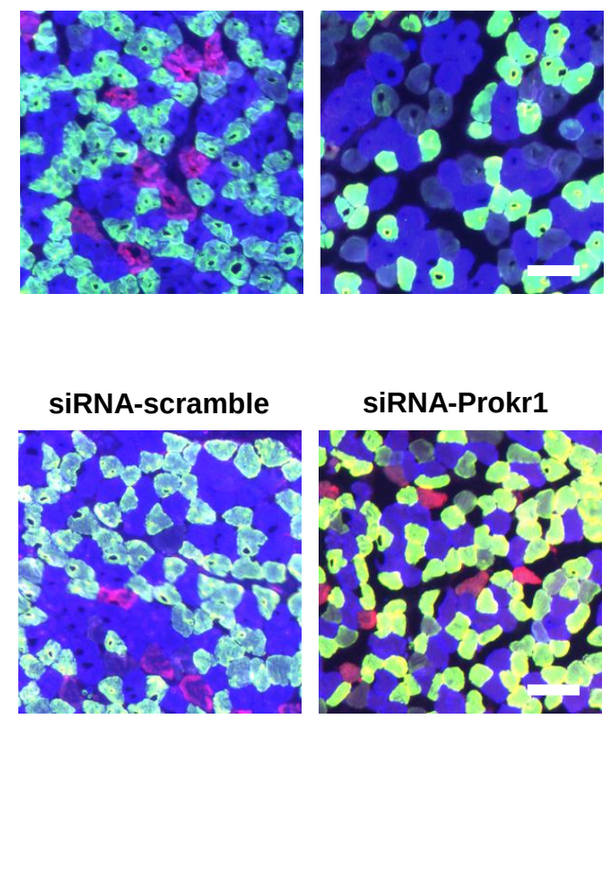

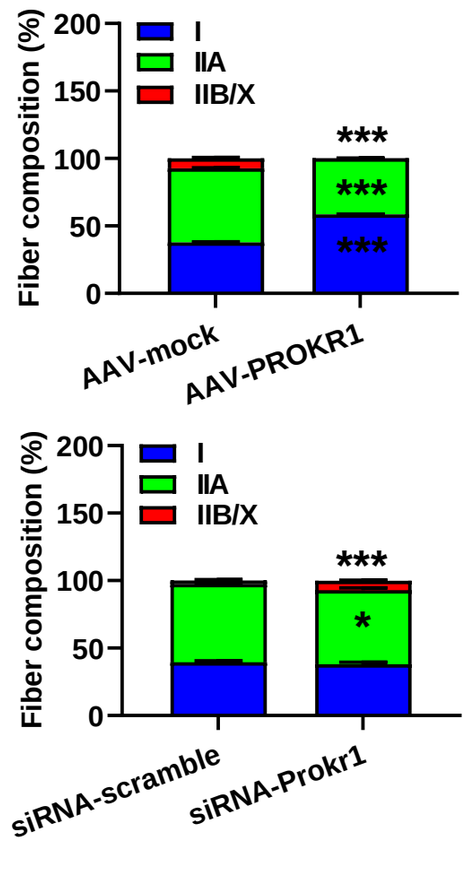

Fig. S25

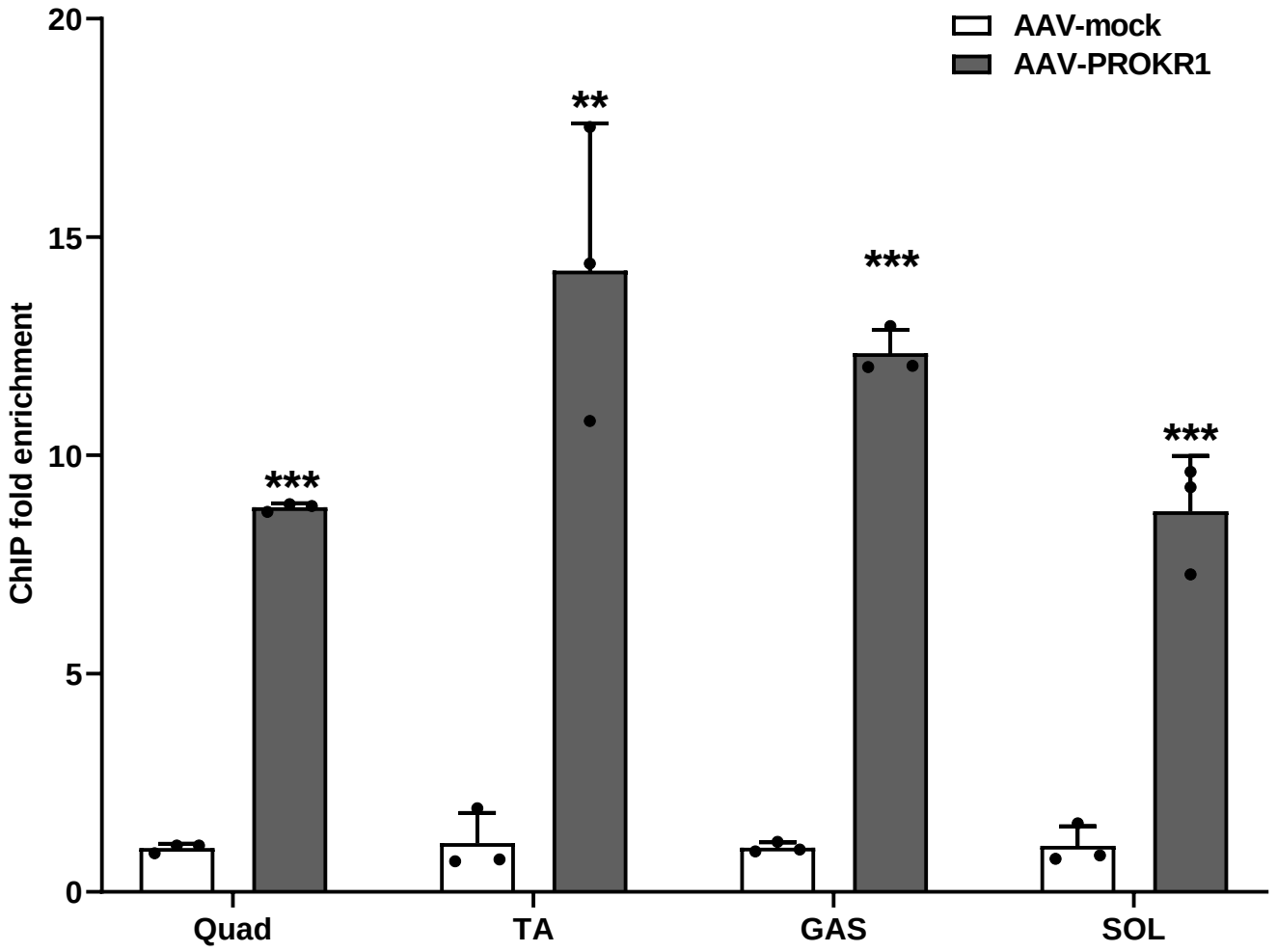
AAV-mock
AAV-PROKR1
ChIP fold enrichment
20
15
10
5
0
***
**
***
***
Quad
TA
GAS
SOL